核理1勉強会 2012.06.07 by A. Tamii

New Method for Precise Determination of the Isovector Giant Quadrupole Resonance in Nuclei

S.S. Henshaw, *et al.*, PRL107, 222501(2011)

New Method for Precise Determination of the Isovector Giant Quadrupole Resonances in Nuclei

S. S. Henshaw,[1] M. W. Ahmed,[1,2] G. Feldman,[3] A. M. Nathan,[4] and H. R. Weller[1]

[1]*Department of Physics and Triangle Universities Nuclear Laboratory, Duke University, TUNL Box 90308, Durham, North Carolina 27708-0308, USA*

[2]*Department of Physics, North Carolina Central University, Durham, North Carolina 27707, USA*

[3]*Department of Physics, George Washington University, Washington, D.C. 20052, USA*

[4]*Department of Physics, University of Illinois, Urbana-Champaign, Illinois 61801, USA*

(Received 29 July 2011; published 23 November 2011)

The intense, nearly monoenergetic, 100% polarized $\vec{\gamma}$-ray beams available at the HI$\vec{\gamma}$S facility, along with the realization that the $E1$-$E2$ interference term that appears in the Compton scattering polarization observable has opposite signs in the forward and backward angles, make it possible to obtain an order-of-magnitude improvement in the determination of the parameters of the isovector giant quadrupole resonance (IVGQR). Accurate IVGQR parameters will lead to a more detailed knowledge of the symmetry energy in the nuclear equation of state which is important for understanding nuclear matter under extreme conditions such as those present in neutron stars. Our new method is demonstrated for the case of ^{209}Bi.

DOI: 10.1103/PhysRevLett.107.222501 PACS numbers: 24.30.Cz, 21.65.Ef, 21.65.Mn, 25.20.Dc

New Method for Precise Determination of the Isovector Giant Quadrupole Resonances in Nuclei

S. S. Henshaw,[1] M. W. Ahmed,[1,2] G. Feldman,[3] A. M. Nathan,[4] and H. R. Weller[1]
[1]Department of Physics and Triangle Universities Nuclear Laboratory, Duke University, TUNL Box 90308, Durham, North Carolina 27708-0308, USA
[2]Department of Physics, North Carolina Central University, Durham, North Carolina 27707, USA
[3]Department of Physics, George Washington University, Washington, D.C. 20052, USA
[4]Department of Physics, University of Illinois, Urbana-Champaign, Illinois 61801, USA
(Received 29 July 2011; published 23 November 2011)

The intense, nearly monoenergetic, 100% polarized $\vec{\gamma}$-ray beams available at the HI$\vec{\gamma}$S facility, along with the realization that the $E1$-$E2$ interference term that appears in the Compton scattering polarization observable has opposite signs in the forward and backward angles, make it possible to obtain an order-of-magnitude improvement in the determination of the parameters of the isovector giant quadrupole resonance (IVGQR). Accurate IVGQR parameters will lead to a more detailed knowledge of the symmetry energy in the nuclear equation of state which is important for understanding nuclear matter under extreme conditions such as those present in neutron stars. Our new method is demonstrated for the case of ^{209}Bi.

DOI: 10.1103/PhysRevLett.107.222501 PACS numbers: 24.30.Cz, 21.65.Ef, 21.65.Mn, 25.20.Dc

・IVGQRのパラメータを決定した。^{209}Bi

・1桁以上の精度の向上

・HI$\vec{\gamma}$S Facility、100%の高強度準単色(直線)偏光γ線を使用

・E1-E2干渉項を見る

→

EoS の対称項、中性子星の性質

E282 at RCNP

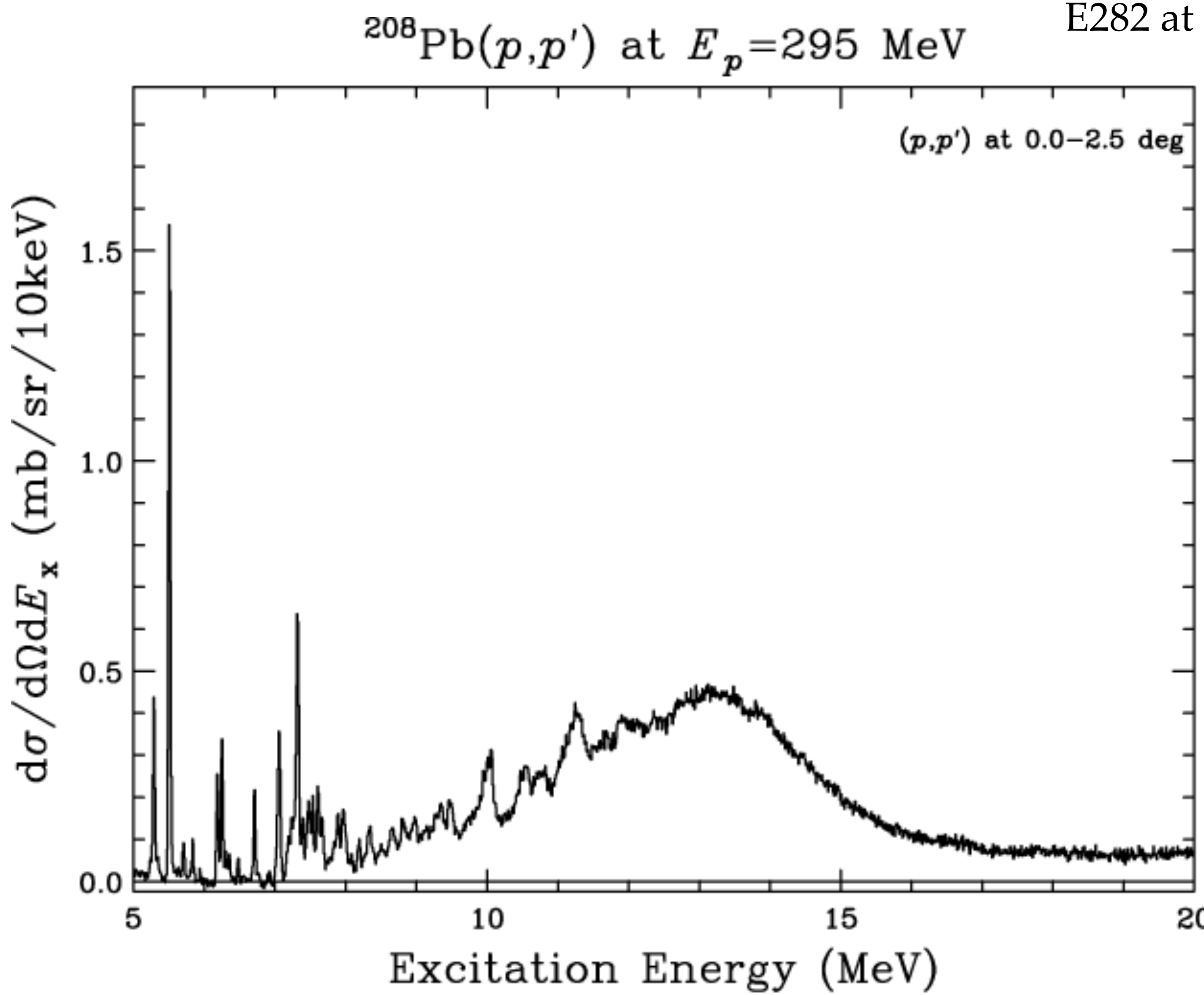

PRL**107**, 062502 (2011)
PRC**85**, 41304(R) (2012)

和則(Sum-Rule)

励起状態の強度を全て積算することで基底状態の
性質と関連付ける

励起状態

励起エネルギー、励起強度,
…

オペレータ
by σ, στ

励起

Sum-Rule

基底状態の性質

基底状態

質量、スピン、パリティ、変形度、…

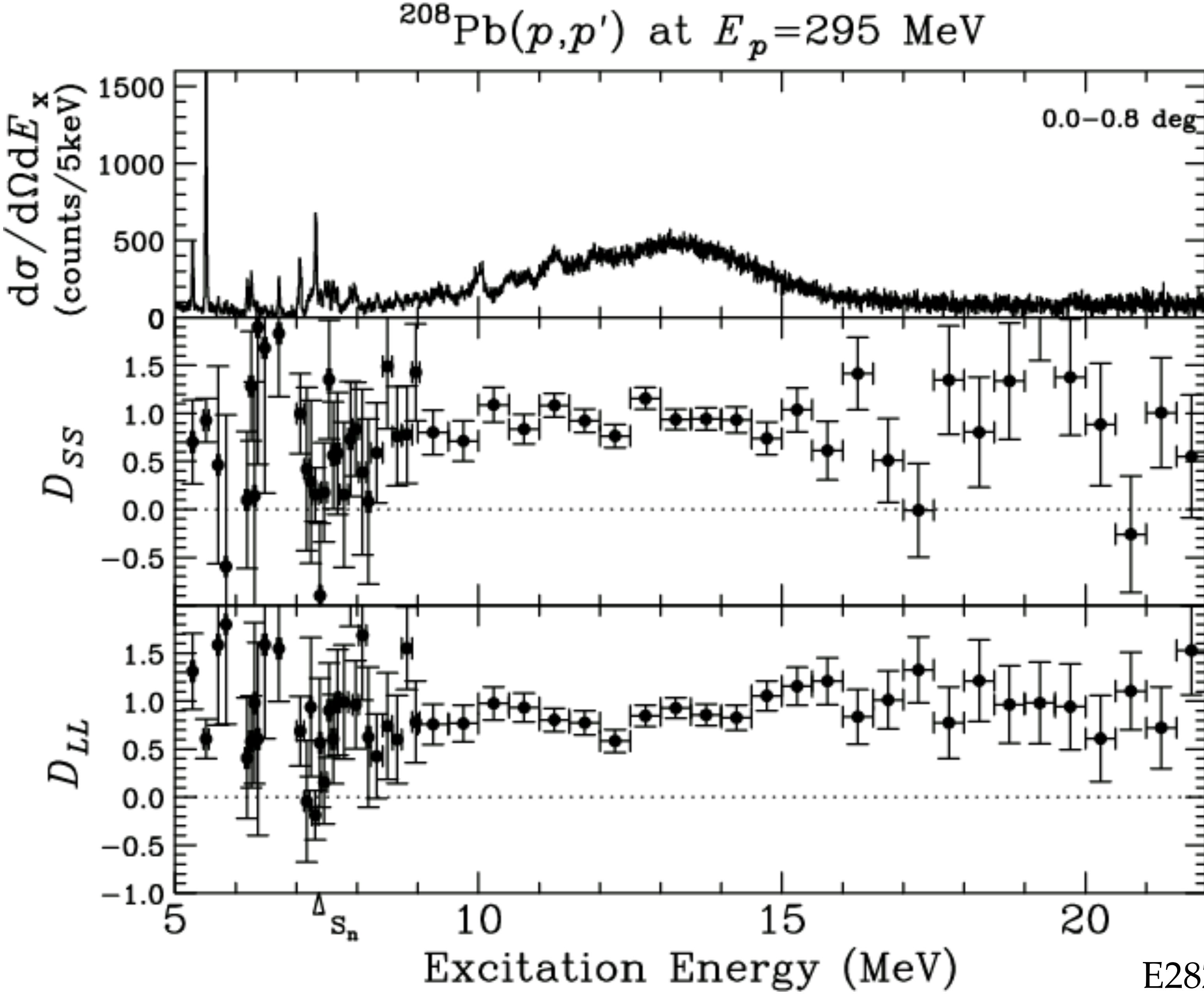
^{208}Pb(p,p′) at E_p=295 MeV
0.0−0.8 deg
dσ/dΩdE_x (counts/5keV)
D_{SS}
D_{LL}
S_n
Excitation Energy (MeV)

E282 at RCNP

Multipole Decomposition

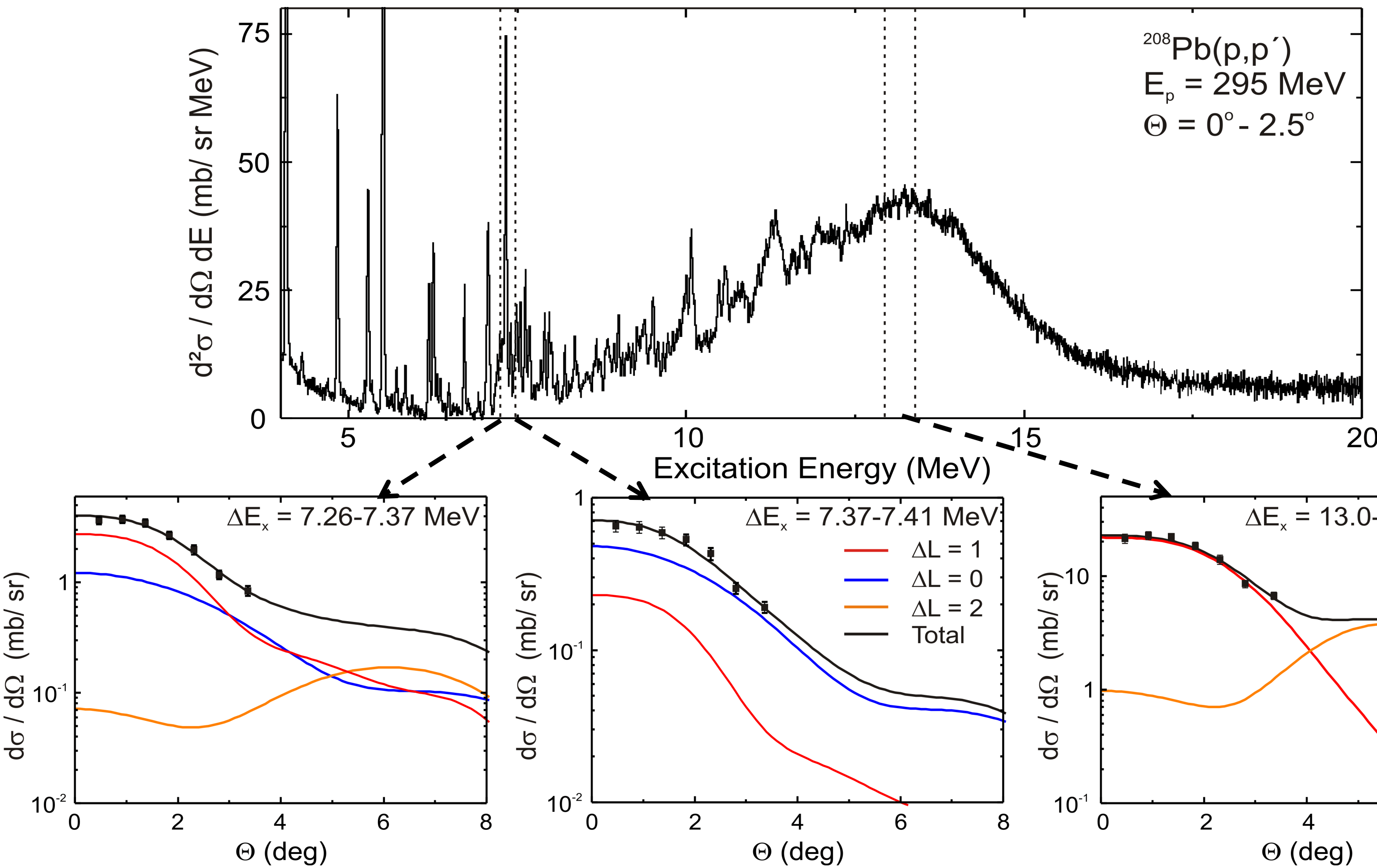

- Neglect of data for Θ>4: (p,p´) response too complex
- Included E1/M1/E2 or E1/M1/E3 (little difference)

E282 at RCNP

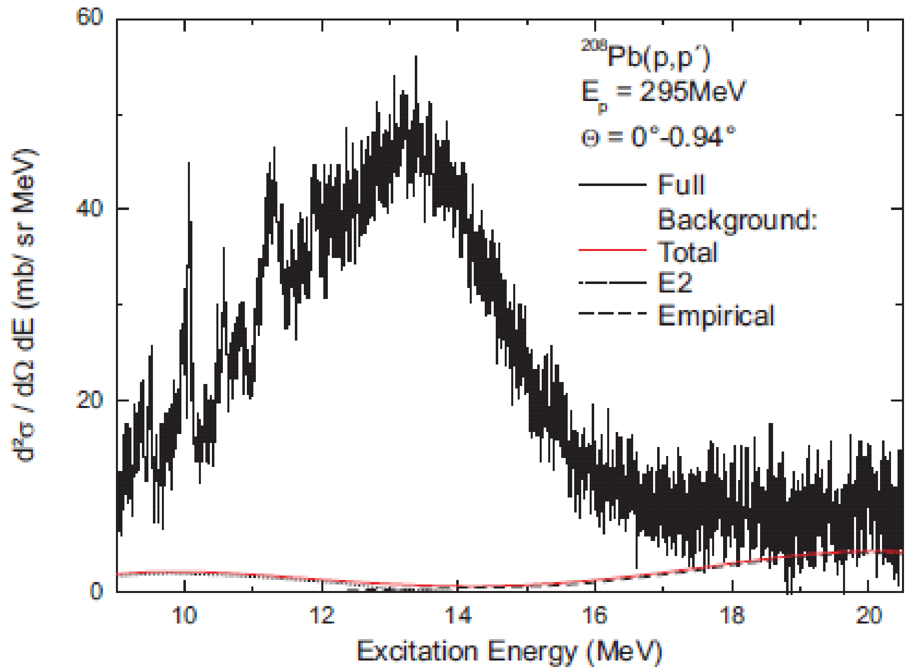

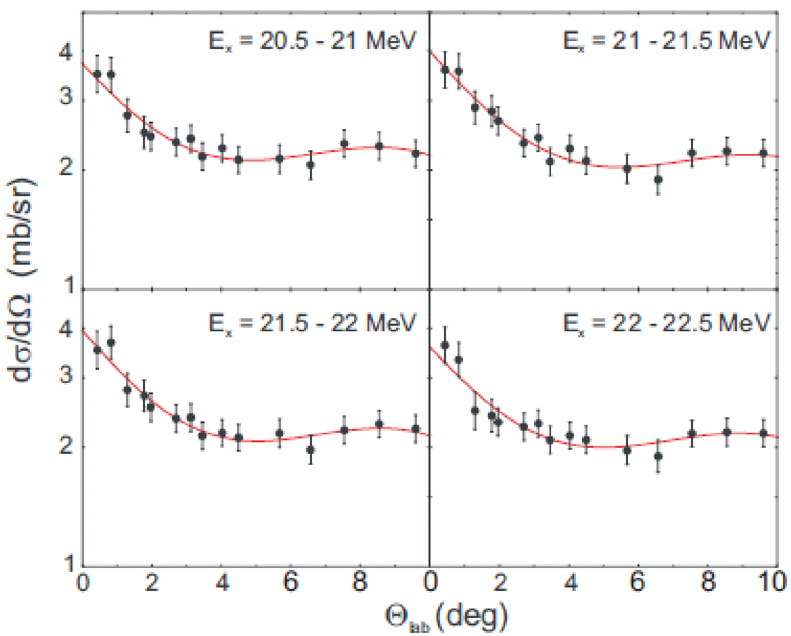

GQR?
suggestion by J. Carter

There also exist data at iThembaLABS.

I. Poltoratska, PhD thesis (2011)

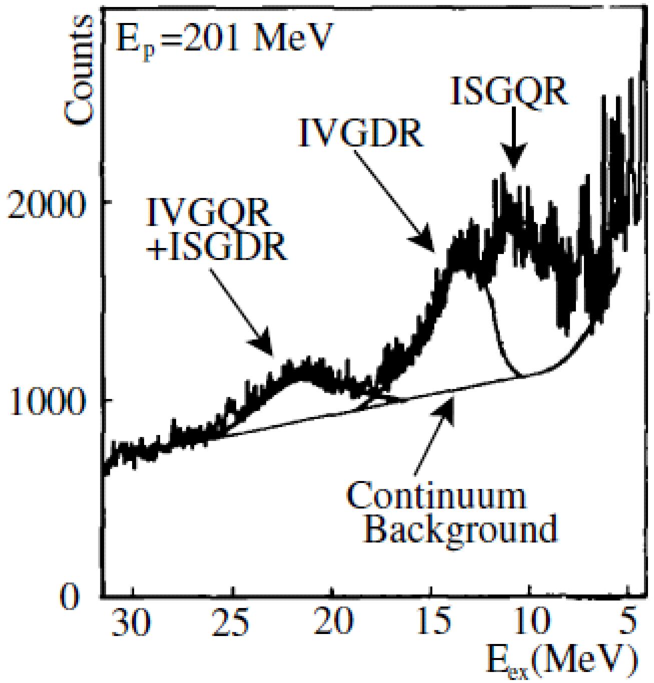

(a) $\theta_{Lab} = 5°$

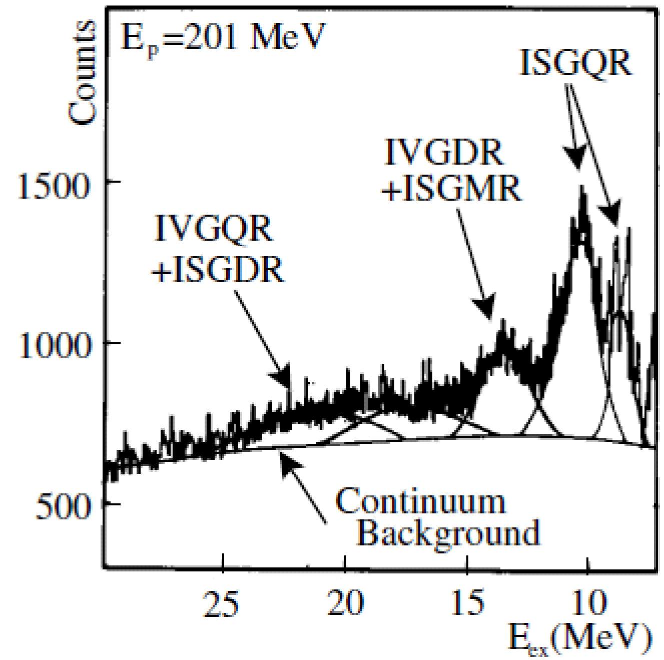

(b) $\theta_{Lab} = 9°$

Figure 1.8: ^{208}Pb(p, p') inelastic scattering spectra at lab angles of $\theta_{Lab} = 5°, 9°$ [Dja82]. The continuum background lineshape is a phenomenological estimation of the quasi-particle scattering. The different resonances are fit to the data with the inclusion of the background. Notice at 17.6 MeV in (b) there is another resonance included to fit the data. The authors argue this is possibly due to high energy octupole resonances but the argument is inconclusive. Identification of the resonance multipolarity and isospin is done via the angular distribution of strength after the spectral fit.

S.S. Henshaw
PhD thesis, 2010

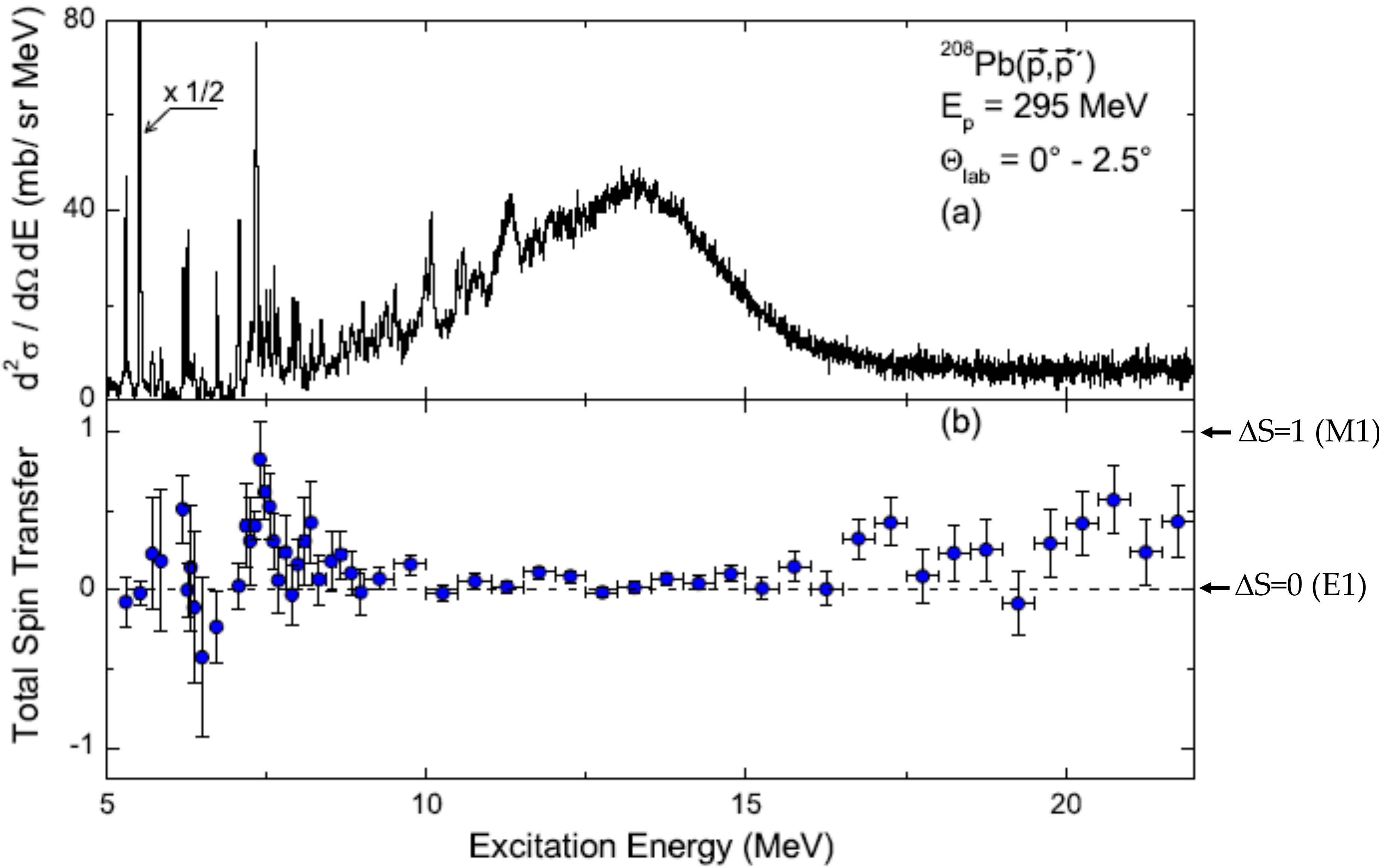

^{208}Pb($\vec{p}$,$\vec{p}'$)
E_p = 295 MeV
Θ_{lab} = 0° - 2.5°
(a)
x 1/2
$d^2\sigma$ / dΩ dE (mb/ sr MeV)
(b)
Total Spin Transfer
← ΔS=1 (M1)
← ΔS=0 (E1)
Excitation Energy (MeV)

E282 at RCNP

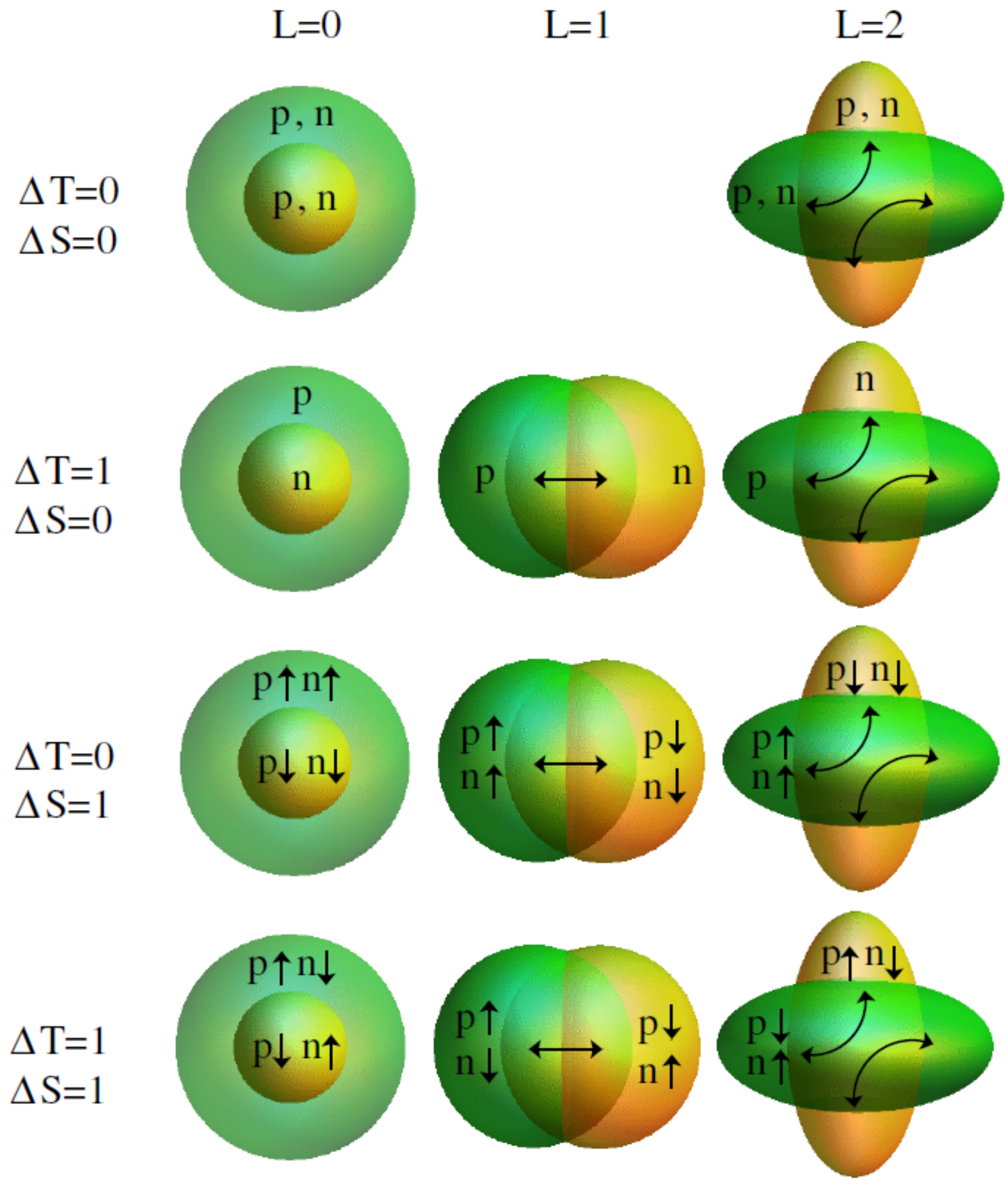

S.S. Henshaw
PhD thesis, 2010

IV Giant Dipole Resonance (IVGDR)

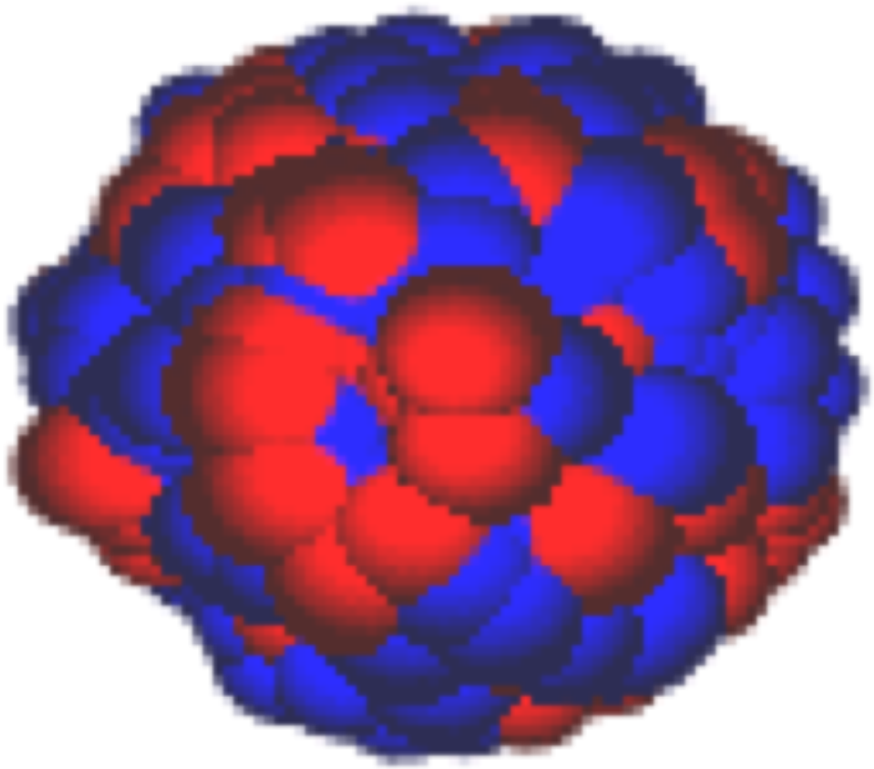

by P. Adrich

Giant Resonance (GQR)

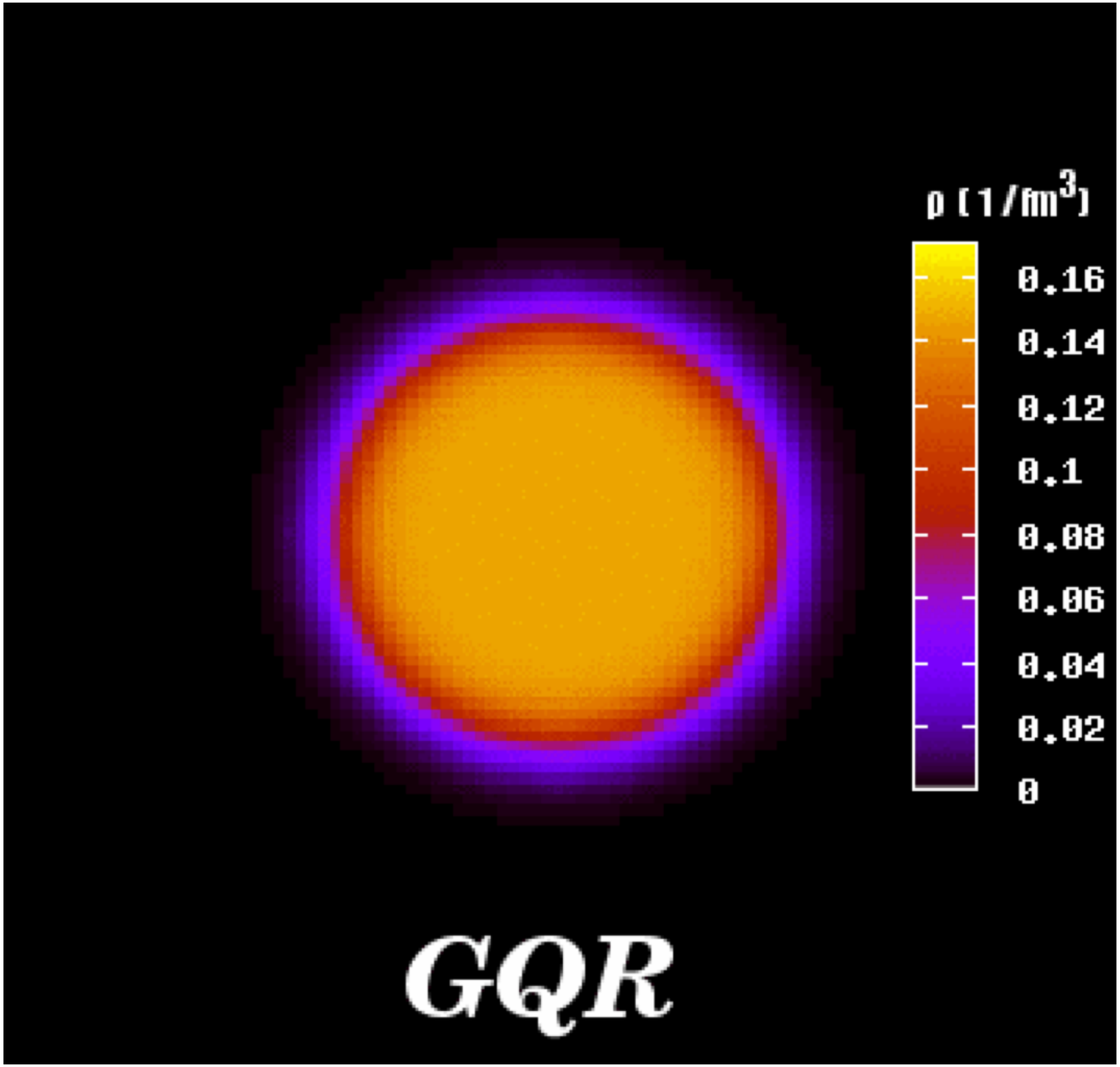

by M. Itoh

IV Giant Quadrupole Resonance (IVGQR)

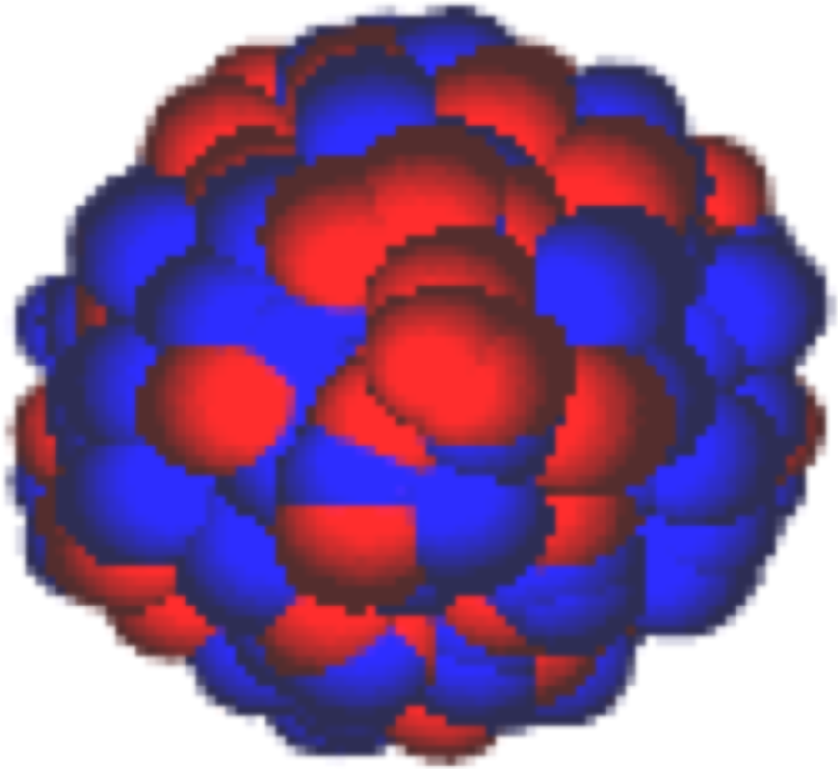

by P. Adrich

Introduction

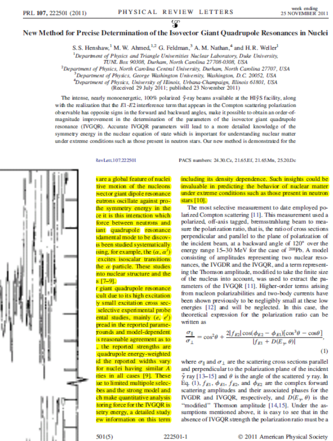
New Method for Precise Determination of the Isovector Giant Quadrupole Resonances in Nuclei

Isovector Giant Dipole Resonance (IVGDR) [2-5]
中性子と陽子の間の相対振動

→核物質の状態方程式(EoS)の
対称項(Symmetry Term)の情報を担う
⇔ 復元力

Isoscalar Giant Quodrupole Resonance (ISGQR) [6]

・1970年代に発見

・(α,α')により系統的に測定されてきた

→核構造、原子核のbulkな性質[7-9]

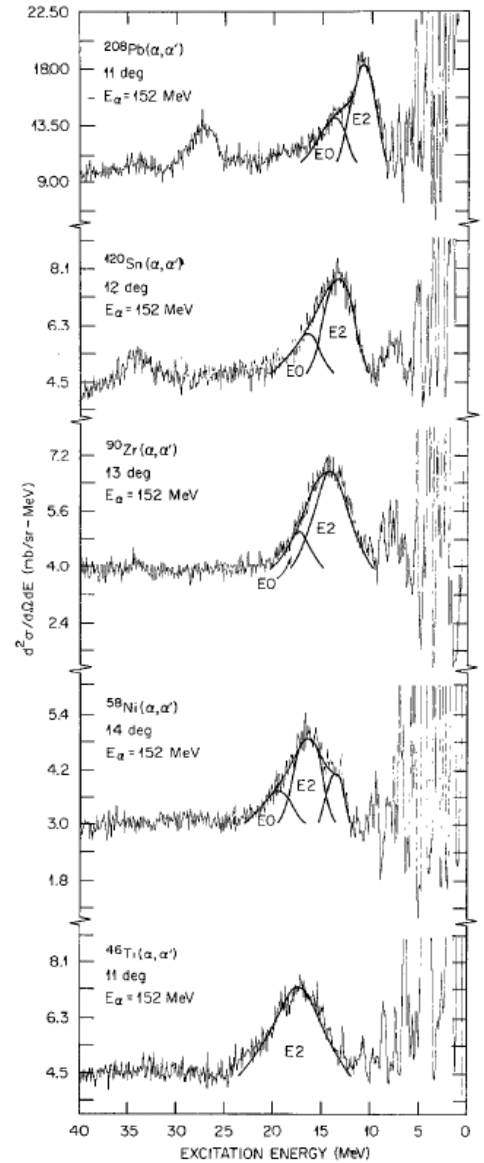

F.E. Bertrand, NPA354,129(1981)

PRL 107, 222501 (2011) PHYSICAL REVIEW LETTERS week ending 25 NOVEMBER 2011

New Method for Precise Determination of the Isovector Giant Quadrupole Resonances in Nuclei

S.S. Henshaw,[1] M. W. Ahmed,[1,2] G. Feldman,[3] A. M. Nathan,[4] and H.R. Weller[1]

[1]*Department of Physics and Triangle Universities Nuclear Laboratory, Duke University, TUNL Box 90308, Durham, North Carolina 27708-0308, USA*
[2]*Department of Physics, North Carolina Central University, Durham, North Carolina 27707, USA*
[3]*Department of Physics, George Washington University, Washington, D.C. 20052, USA*
[4]*Department of Physics, University of Illinois, Urbana-Champaign, Illinois 61801, USA*

(Received 29 July 2011; published 23 November 2011)

The intense, nearly monoenergetic, 100% polarized $\vec{\gamma}$-ray beams available at the HI$\vec{\gamma}$S facility, along with the realization that the $E1$-$E2$ interference term that appears in the Compton scattering polarization observable has opposite signs in the forward and backward angles, make it possible to obtain an order-of-magnitude improvement in the determination of the parameters of the isovector giant quadrupole resonance (IVGQR). Accurate IVGQR parameters will lead to a more detailed knowledge of the symmetry energy in the nuclear equation of state which is important for understanding nuclear matter under extreme conditions such as those present in neutron stars. Our new method is demonstrated for the case of ^{209}Bi.

DOI: 10.1103/PhysRevLett.107.222501 PACS numbers: 24.30.Cz, 21.65.Ef, 21.65.Mn, 25.20.Dc

Giant multipole resonances are a global feature of nuclei which arise from the collective motion of the nucleons inside the nucleus [1]. The isovector giant dipole resonance (IVGDR) [2–5], for which neutrons oscillate against protons, provides insight into the symmetry energy in the nuclear equation of state since it is this interaction which gives rise to the restoring force between neutrons and protons. The isoscalar giant quadrupole resonance (ISGQR) [6] was the next fundamental mode to be discovered in the early 1970s and has been studied systematically over the nuclear mass range using, for example, the (α, α') probe, which preferentially excites isoscalar transitions due to the $T = 0$ nature of the α particle. These studies have provided new insights into nuclear structure and the bulk properties of the nucleus [7–9].

The study of the isovector giant quadrupole resonance (IVGQR) has been more difficult due to its high excitation energy, large width, relatively small excitation cross section, and the lack of a highly selective experimental probe [1]. The results of experimental studies, mainly (e, e') investigations, show a large spread in the reported parameters as a result of large backgrounds and model-dependent corrections [1]. While there is reasonable agreement as to the location of the IVGQR, the reported strengths are between 0 and 1.4 isovector quadrupole energy-weighted sum rules (IVQEWSRs) and the reported widths vary between 3.5 and 10 MeV for nuclei having similar A values, with large uncertainties in all cases [9]. These inconsistencies come about due to limited multipole selectivity in the experimental probes and the strong model and theoretical dependencies which make quantitative analysis problematic [9]. Since the restoring force for the IVGQR is also determined by the symmetry energy, a detailed study of this mode will provide new information on this term including its density dependence. Such insights could be invaluable in predicting the behavior of nuclear matter under extreme conditions such as those present in neutron stars [10].

The most selective measurement to date employed polarized Compton scattering [11]. This measurement used a polarized, off-axis tagged, bremsstrahlung beam to measure the polarization ratio, that is, the ratio of cross sections perpendicular and parallel to the plane of polarization of the incident beam, at a backward angle of 120° over the energy range 15–30 MeV for the case of ^{208}Pb. A model consisting of amplitudes representing two nuclear resonances, the IVGDR and the IVGQR, and a term representing the Thomson amplitude, modified to take the finite size of the nucleus into account, was used to extract the parameters of the IVGQR [11]. Higher-order terms arising from nucleon polarizabilities and two-body currents have been shown previously to be negligibly small at these low energies [12] and will be neglected. In this case, the theoretical expression for the polarization ratio can be written as

$$\frac{\sigma_\parallel}{\sigma_\perp} = \cos^2\theta + \frac{2|f_{E2}|\cos(\phi_{E2} - \phi_{E1})[\cos^3\theta - \cos\theta]}{|f_{E1} + D(E_\gamma, \theta)|}, \quad (1)$$

where $\sigma_\parallel$ and $\sigma_\perp$ are the scattering cross sections parallel and perpendicular to the polarization plane of the incident $\vec{\gamma}$ ray [13–15] and θ is the angle of the scattered γ ray. In Eq. (1), f_{E1}, ϕ_{E1}, f_{E2}, and ϕ_{E2} are the complex forward scattering amplitudes and their associated phases for the IVGDR and IVGQR, respectively, and $D(E_\gamma, \theta)$ is the "modified" Thomson amplitude [14,15]. Under the assumptions mentioned above, it is easy to see that in the absence of IVGQR strength the polarization ratio must be a

0031-9007/11/107(22)/222501(5) 222501-1 © 2011 American Physical Society

Introduction

Isovector Giant Qudrupole Resonance (IVGQR) [2-5]
→核物質の状態方程式(EoS)の対称項（Symmetry Term）の情報を担う
⇔ 復元力

密度依存性など　→中性子星などの極限状態での核物質の性質

これまで測定が困難であった（よいプローブの欠如）

・高励起エネルギー

・大きい幅

・比較小さい励起断面積

電子散乱により主に調べられてきた。

・得られたパラメータの精度が悪い[9]

←大きいバックグラウンド、モデル依存の補正などが原因

・Isovector Quadrupole Energy-Weighted Sum-Rule (IVQEWSR)
の0-1.4倍程度の強度

・3.5-10 MeV の幅

$$\int \frac{\sigma_\gamma^{E2}(E)}{E^2} dE = \frac{\pi^2}{3}\frac{e^2}{\hbar c}\frac{NZ}{M_n c^2 A}\langle r^2 \rangle$$

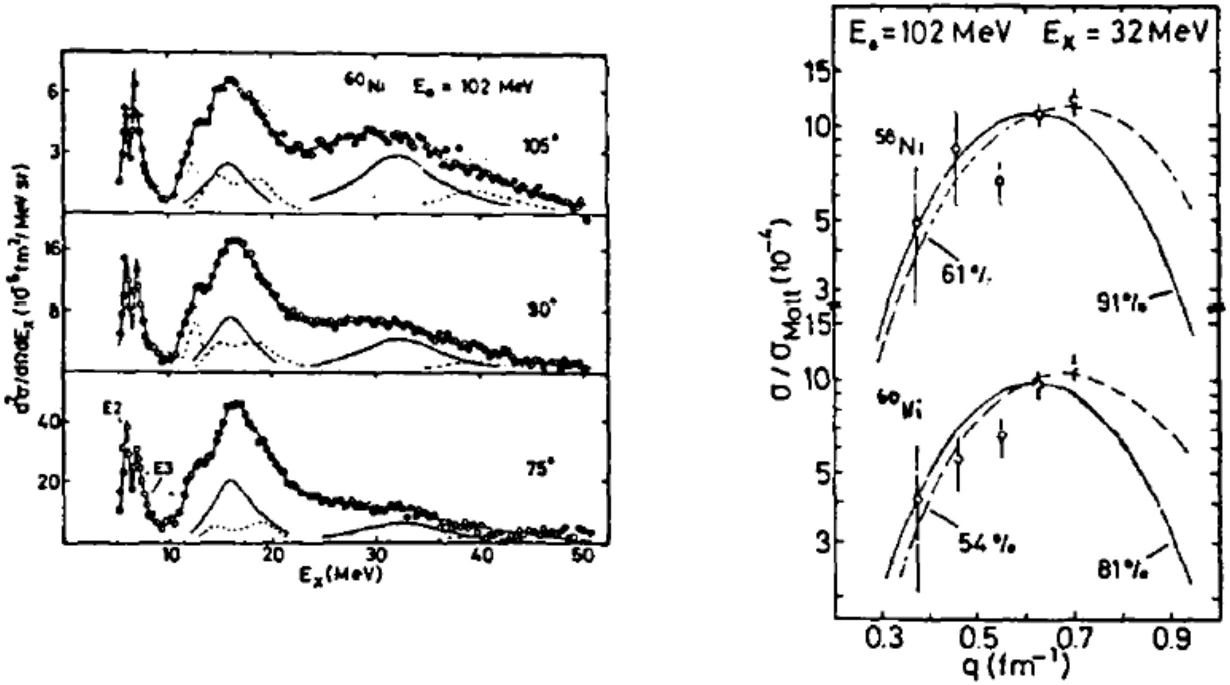

Fig. 10. Left; Inelastic electron scattering from ^{60}Ni. The broad pea
MeV of excitation is assigned as isovector quadrupole resonance (ref. 1
Right; Form factors for the isovector E2 states observed (ref. 13) in ^{5}
^{60}Ni. The solid curve is for the Goldhaber-Teller model while the dash
is from the Myers-Swiatecki prescription.

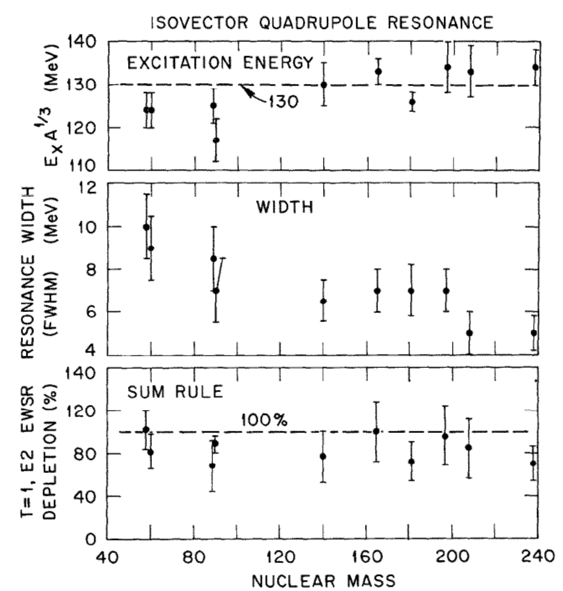

Fig. 11. Systematics of the excitation energy, width and sum rule depletion of the isovector giant quadrupole resonance. The data are from ref. 14.

F.E. Bertrand, NPA354,129(1981)

Methodology


PRL **107,** 222501 (2011) PHYSICAL REVIEW LETTERS week ending 25 NOVEMBER 2011

New Method for Precise Determination of the Isovector Giant Quadrupole Resonances in Nuclei

S. S. Henshaw,[1] M. W. Ahmed,[1,2] G. Feldman,[3] A. M. Nathan,[4] and H. R. Weller[1]
[1]*Department of Physics and Triangle Universities Nuclear Laboratory, Duke University, TUNL Box 90308, Durham, North Carolina 27708-0308, USA*
[2]*Department of Physics, North Carolina Central University, Durham, North Carolina 27707, USA*
[3]*Department of Physics, George Washington University, Washington, D.C. 20052, USA*
[4]*Department of Physics, University of Illinois, Urbana-Champaign, Illinois 61801, USA*
(Received 29 July 2011; published 23 November 2011)

The intense, nearly monoenergetic, 100% polarized $\vec{\gamma}$-ray beams available at the HI$\vec{\gamma}$S facility, along with the realization that the $E1$-$E2$ interference term that appears in the Compton scattering polarization observable has opposite signs in the forward and backward angles, make it possible to obtain an order-of-magnitude improvement in the determination of the parameters of the isovector giant quadrupole resonance (IVGQR). Accurate IVGQR parameters will lead to a more detailed knowledge of the symmetry energy in the nuclear equation of state which is important for understanding nuclear matter under extreme conditions such as those present in neutron stars. Our new method is demonstrated for the case of ^{209}Bi.

DOI: 10.1103/PhysRevLett.107.222501 PACS numbers: 24.30.Cz, 21.65.Ef, 21.65.Mn, 25.20.Dc

Giant multipole resonances are a global feature of nuclei which arise from the collective motion of the nucleons inside the nucleus [1]. The isovector giant dipole resonance (IVGDR) [2–5], for which neutrons oscillate against protons, provides insight into the symmetry energy in the nuclear equation of state since it is this interaction which gives rise to the restoring force between neutrons and protons. The isoscalar giant quadrupole resonance (ISGQR) [6] was the next fundamental mode to be discovered in the early 1970s and has been studied systematically over the nuclear mass range using, for example, the (α, α') probe, which preferentially excites isoscalar transitions due to the $T = 0$ nature of the α particle. These studies have provided new insights into nuclear structure and the bulk properties of the nucleus [7–9].

The study of the isovector giant quadrupole resonance (IVGQR) has been more difficult due to its high excitation energy, large width, relatively small excitation cross section, and the lack of a highly selective experimental probe [1]. The results of experimental studies, mainly (e, e') investigations, show a large spread in the reported parameters as a result of large backgrounds and model-dependent corrections [1]. While there is reasonable agreement as to the location of the IVGQR, the reported strengths are between 0 and 1.4 isovector quadrupole energy-weighted sum rules (IVQEWSRs) and the reported widths vary between 3.5 and 10 MeV for nuclei having similar A values, with large uncertainties in all cases [9]. These inconsistencies come about due to limited multipole selectivity in the experimental probes and the strong model and theoretical dependencies which make quantitative analysis problematic [9]. Since the restoring force for the IVGQR is also determined by the symmetry energy, a detailed study of this mode will provide new information on this term including its density dependence. Such insights could be invaluable in predicting the behavior of nuclear matter under extreme conditions such as those present in neutron stars [10].

The most selective measurement to date employed polarized Compton scattering [11]. This measurement used a polarized, off-axis tagged, bremsstrahlung beam to measure the polarization ratio, that is, the ratio of cross sections perpendicular and parallel to the plane of polarization of the incident beam, at a backward angle of 120° over the energy range 15–30 MeV for the case of ^{208}Pb. A model consisting of amplitudes representing two nuclear resonances, the IVGDR and the IVGQR, and a term representing the Thomson amplitude, modified to take the finite size of the nucleus into account, was used to extract the parameters of the IVGQR [11]. Higher-order terms arising from nucleon polarizabilities and two-body currents have been shown previously to be negligibly small at these low energies [12] and will be neglected. In this case, the theoretical expression for the polarization ratio can be written as

$$\frac{\sigma_\parallel}{\sigma_\perp} = \cos^2\theta + \frac{2|f_{E2}|\cos(\phi_{E2} - \phi_{E1})[\cos^3\theta - \cos\theta]}{|f_{E1} + D(E_\gamma, \theta)|}, \quad (1)$$

where $\sigma_\parallel$ and $\sigma_\perp$ are the scattering cross sections parallel and perpendicular to the polarization plane of the incident $\vec{\gamma}$ ray [13–15] and θ is the angle of the scattered γ ray. In Eq. (1), f_{E1}, ϕ_{E1}, f_{E2}, and ϕ_{E2} are the complex forward scattering amplitudes and their associated phases for the IVGDR and IVGQR, respectively, and $D(E_\gamma, \theta)$ is the "modified" Thomson amplitude [14,15]. Under the assumptions mentioned above, it is easy to see that in the absence of IVGQR strength the polarization ratio must be a

0031-9007/11/107(22)/222501(5) 222501-1 © 2011 American Physical Society

Polarized Compton Scattering [11]
^{208}Pb, Dale, Laszewski, and Alarcon @ Illinois

- off-axis tagged bremsstrahlung (polarized-gamma)
- $\sigma_\parallel, \sigma_\perp$:偏光面(磁界方向)に対して並行、反並行
- 後方角度: 120 deg
- 15-30 MeV
- IVGDR(E1) and IVGQR(E2) (偏光)amplitude
- Thomson amplitude ... 原子核の有限サイズの効果をとりいれる。
- nucleon polarizability, two-body currents の効果は十分小さい [12]

$$S^{fi}_{\lambda'\lambda} = \left[-\frac{Ze^2}{M_N c^2} F_1(q) + \frac{NZ}{A}\frac{e^2}{M_N c^2} \right] \hat{\epsilon}_{\lambda'} \cdot \hat{\epsilon}_{\lambda} \quad (2.5)$$

$$F_1(q) = \int \rho(r) e^{i\vec{q}\cdot\vec{r}} d^3 r. \quad (2.6)$$

$D(E_\gamma, \theta)$

Off-Axis Tagged Bremsstrahlung Gamma Source

Illinois, Urbanna-Champaign

R.M. Laszewski et al., NIMA228, 334(1985)

Sn近傍のM1の励起強度分布測定に大きく貢献

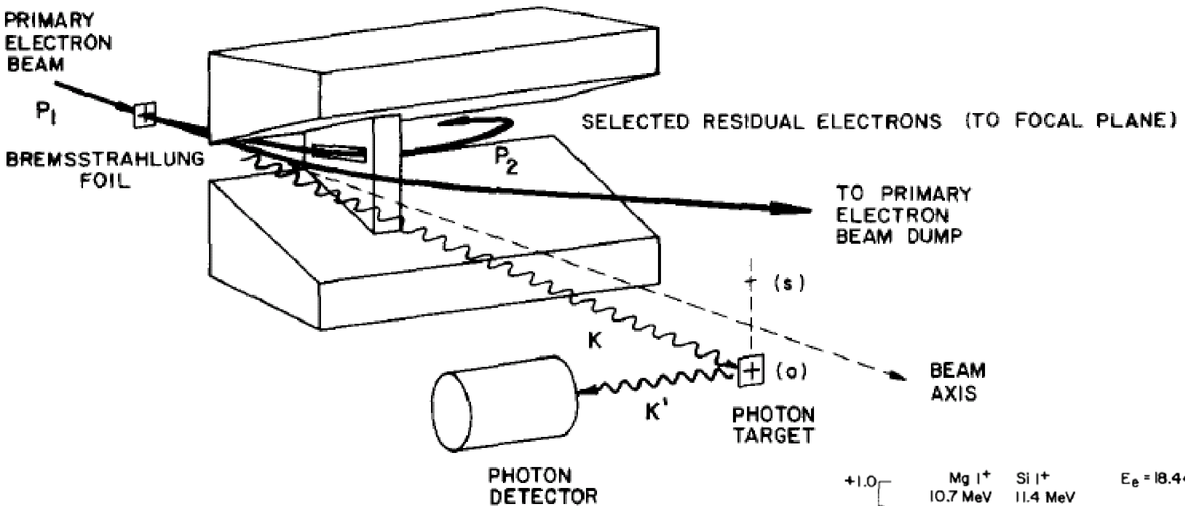

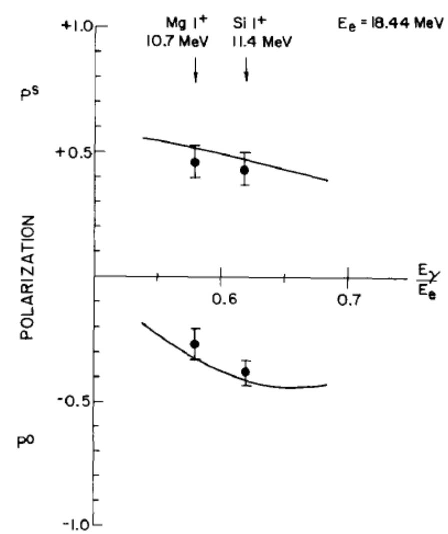

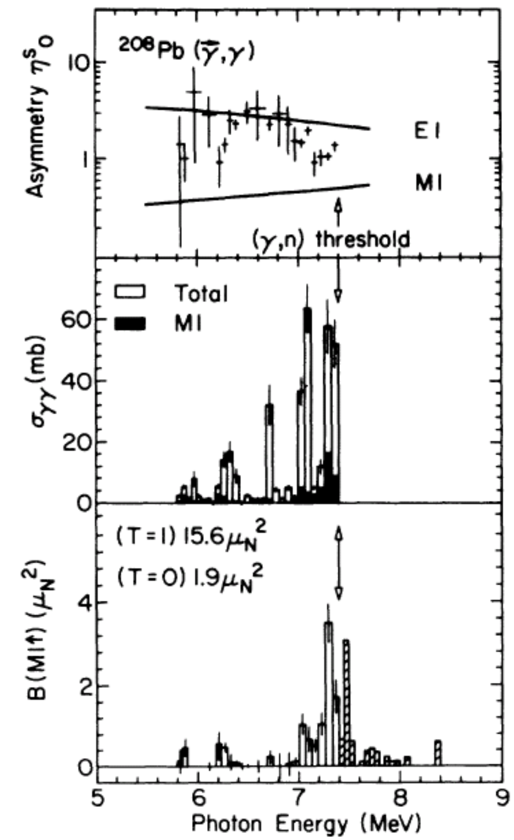

Off-axis Bremsstrahlung

ELBE, Dresden-Rossendorf

近年精力的にデータを出している。

$$\theta = \frac{m_0 c^2}{E_e}$$

≦20 MeV
1mA
26-260MHz, 5ps

Nb 3.5mg/cm2
2mm collimator

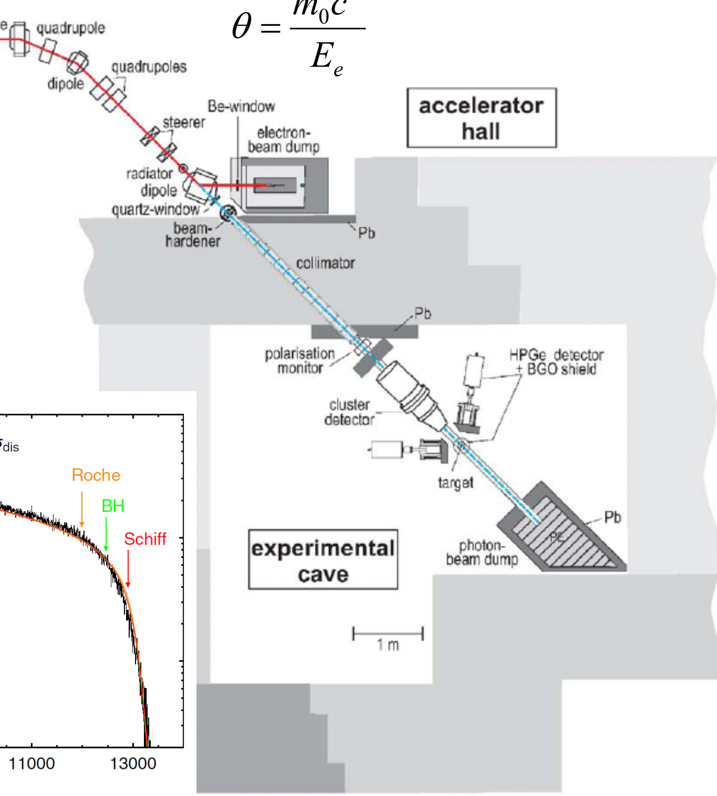

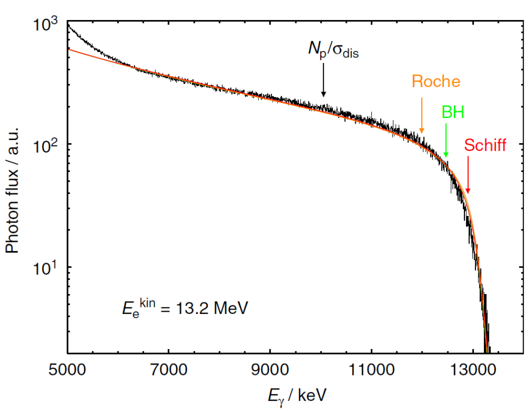

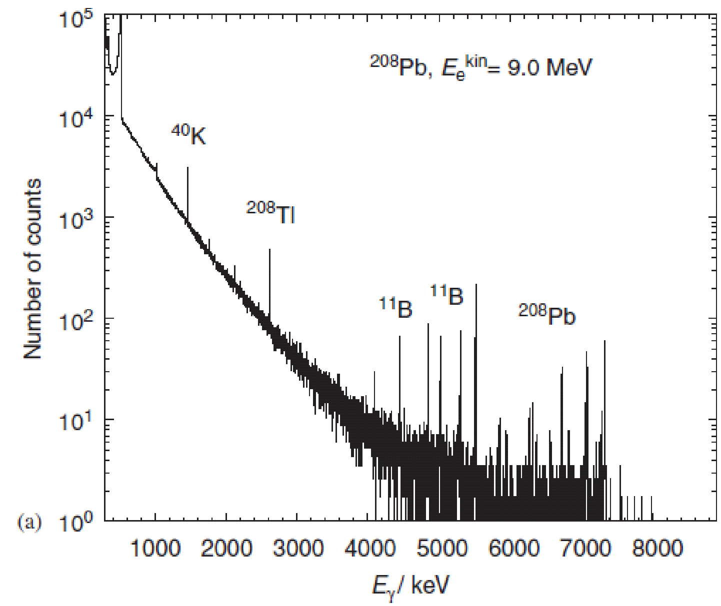

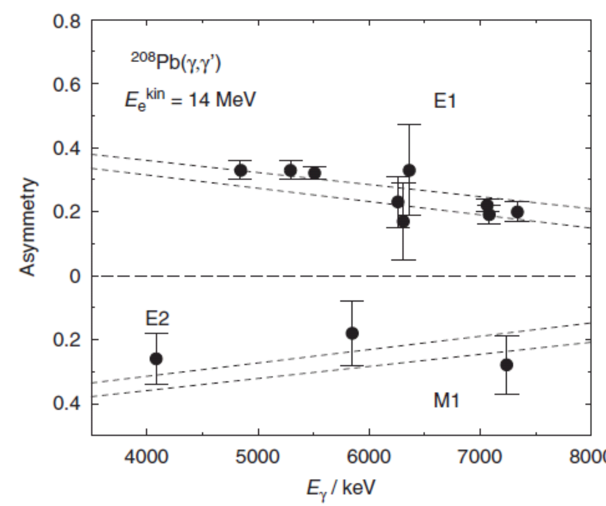

R. Schwengner et al., NIMA555, 211(2005)

Off-axis Bremsstrahlung

Govaert et al., NIMA337, 265(1994)

Gent

≦12 MeV
350μA
4 kHz

Al 25μm
7mm Fe+Pb
collimator

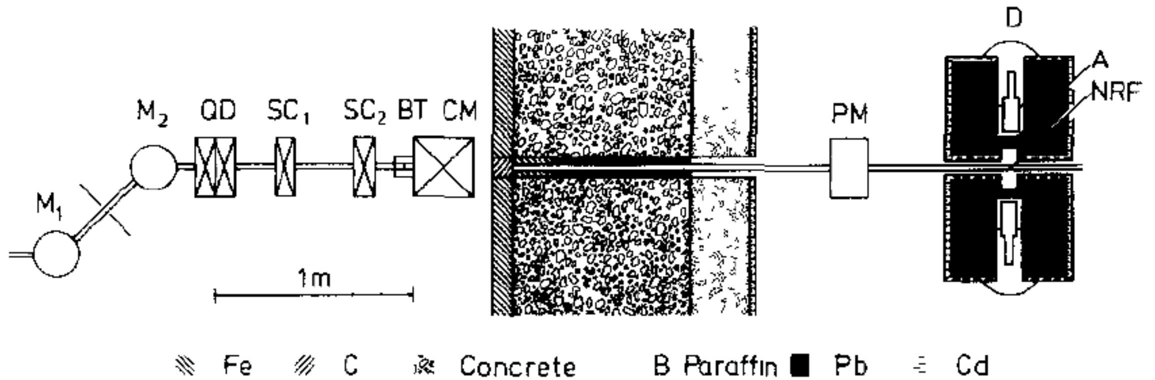

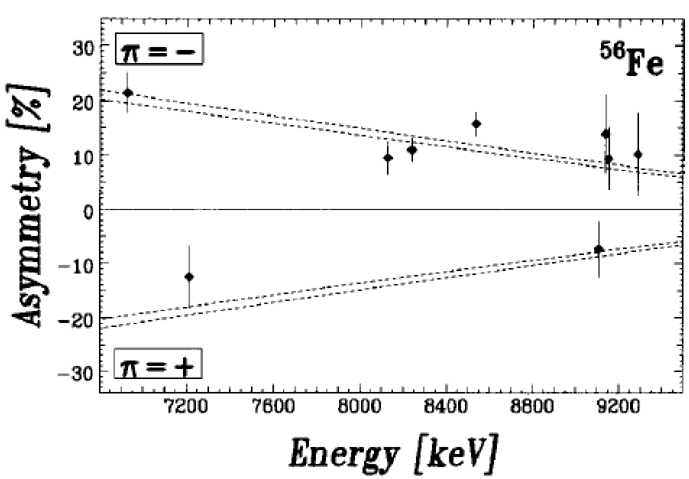

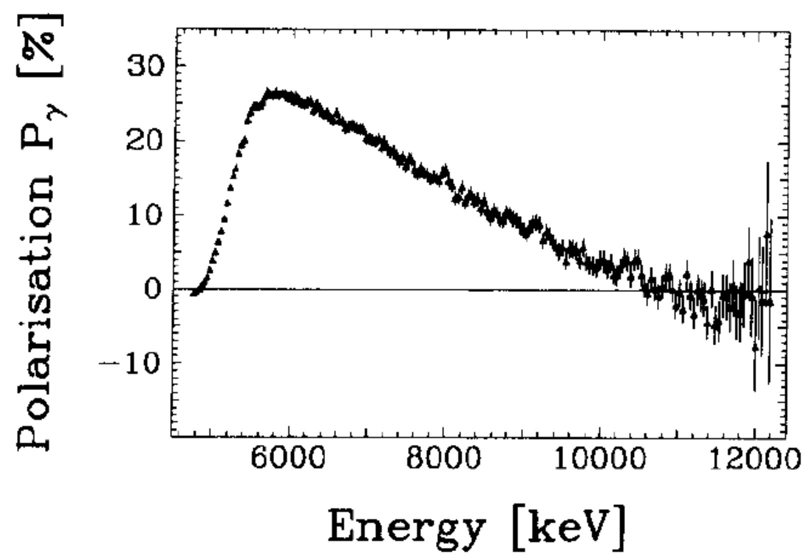

Methodology


PRL 107, 222501 (2011) PHYSICAL REVIEW LETTERS week ending 25 NOVEMBER 2011

New Method for Precise Determination of the Isovector Giant Quadrupole Resonances in Nuclei

1/4

$\mp\frac{3}{8}$

$$\frac{\sigma_{\parallel}}{\sigma_{\perp}} = \cos^2\theta + \frac{2|f_{E2}|\cos(\phi_{E2}-\phi_{E1})[\cos^3\theta - \cos\theta]}{|f_{E1} + D(E_\gamma,\theta)|}, \tag{1}$$

$\sigma_{\parallel}, \sigma_{\perp}$ ：偏光面（磁界方向）に対して並行、反並行

θ：散乱角

f_{E1}, f_{E2}:　散乱振幅

ϕ_{E1}, ϕ_{E2}:　位相

D: Modified Thomson Amplitude [14,15]

$f_{E2}=0$ の時　$\frac{\sigma_{\parallel}}{\sigma_{\perp}} = \cos^2\theta$

ϕ_{E1}, $\phi_{E2}=90°$　の時　$\frac{\sigma_{\parallel}}{\sigma_{\perp}} = \cos^2\theta$

D.S. Dale et al., PRL68, 3507(1992)

Off-axis Bremsstrahlung, ^{208}Pb

Illinois, Urbanna-Champaign

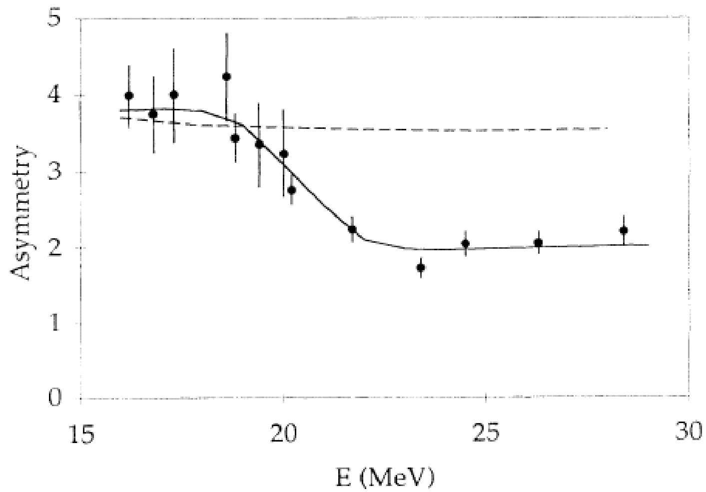

FIG. 1. ^{208}Pb experimental polarization asymmetries at 120°. The asymmetry expected in the absence of an IVGQR is shown by the dashed line. The solid curve indicates the best fit of the $E1$-$E2$ interference to both the polarization asymmetry and the total photoabsorption.

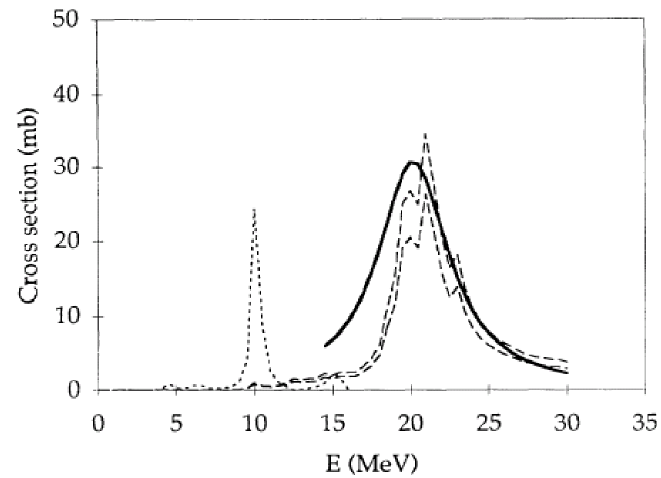

FIG. 2. The distribution of $E2$ transition strength from the present work (solid curve) together with a continuum RPA calculation of isoscalar (dots) and isovector (dashes) $E2$ strength from Ref. [42]. For comparison, the RPA isovector $E2$ is also shown with a 30% enhancement.

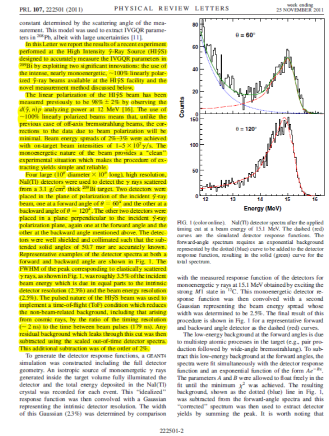

PRL **107,** 222501 (2011) PHYSICAL REVIEW LETTERS week ending 25 NOVEMBER 2011

constant determined by the scattering angle of the measurement. This model was used to extract IVGQR parameters in ^{208}Pb, albeit with large uncertainties [11].

In this Letter we report the results of a recent experiment performed at the High Intensity $\vec{\gamma}$-Ray Source (HI$\vec{\gamma}$S) designed to accurately measure the IVGQR parameters in ^{209}Bi by exploiting two significant innovations: the use of the intense, nearly monoenergetic, ~100% linearly polarized $\vec{\gamma}$-ray beams available at the HI$\vec{\gamma}$S facility and the novel measurement method discussed below.

The linear polarization of the HI$\vec{\gamma}$S beam has been measured previously to be 98% ± 2% by observing the $d(\vec{\gamma}, n)p$ analyzing power at 12 MeV [16]. The use of ~100% linearly polarized beams means that, unlike the previous case of off-axis bremsstrahlung beams, the corrections to the data due to beam polarization will be minimal. Beam energy spreads of 2%–3% were achieved with on-target beam intensities of $1–5 \times 10^7$ γ/s. The monoenergetic nature of the beam provides a "clean" experimental situation which makes the procedure of extracting yields simple and reliable.

Four large (10″ diameter × 10″ long), high resolution, NaI(Tl) detectors were used to detect the γ rays scattered from a 3.1 g/cm^2 thick ^{209}Bi target. Two detectors were placed in the plane of polarization of the incident $\vec{\gamma}$-ray beam, one at a forward angle of $\theta = 60°$ and the other at a backward angle of $\theta = 120°$. The other two detectors were placed in a plane perpendicular to the incident $\vec{\gamma}$-ray polarization plane, again one at the forward angle and the other at the backward angle mentioned above. The detectors were well shielded and collimated such that the subtended solid angles of 50.7 msr are accurately known. Representative examples of the detector spectra at both a forward and backward angle are shown in Fig. 1. The FWHM of the peak corresponding to elastically scattered γ rays, as shown in Fig. 1, was roughly 3.5% of the incident beam energy which is due in equal parts to the intrinsic detector resolution (2.3%) and the beam energy resolution (2.5%). The pulsed nature of the HI$\vec{\gamma}$S beam was used to implement a time-of-flight (ToF) condition which reduces the non-beam-related background, including that arising from cosmic rays, by the ratio of the timing resolution (~ 2 ns) to the time between beam pulses (179 ns). Any residual background which leaks through this cut was then subtracted using the scaled out-of-time detector spectra. This additional subtraction was of the order of 2%.

To generate the detector response functions, a GEANT4 simulation was constructed including the full detector geometry. An isotropic source of monoenergetic γ rays generated inside the target volume fully illuminated the detector and the total energy deposited in the NaI(Tl) crystal was recorded for each event. This "idealized" response function was then convolved with a Gaussian representing the intrinsic detector resolution. The width of this Gaussian (2.3%) was determined by comparison

FIG. 1 (color online). NaI(Tl) detector spectra after the applied timing cut at a beam energy of 15.1 MeV. The dashed (red) curves are the simulated detector response functions. The forward-angle spectrum requires an exponential background represented by the dotted (blue) curve to be added to the detector response function, resulting in the solid (green) curve for the total spectrum.

with the measured response function of the detectors for monoenergetic γ rays at 15.1 MeV obtained by exciting the strong $M1$ state in ^{12}C. This monoenergetic detector response function was then convolved with a second Gaussian representing the beam energy spread whose width was determined to be 2.5%. The final result of this procedure is shown in Fig. 1 for a representative forward and backward angle detector as the dashed (red) curves.

The low-energy background at the forward angles is due to multistep atomic processes in the target (e.g., pair production followed by wide-angle bremsstrahlung). To subtract this low-energy background at the forward angles, the spectra were fit simultaneously with the detector response function and an exponential function of the form Ae^{-Bx}. The parameters A and B were allowed to float freely in the fit until the minimum χ^2 was achieved. The resulting background, shown as the dotted (blue) line in Fig. 1, was subtracted from the forward-angle spectra and this "corrected" spectrum was then used to extract detector yields by summing the peak. It is worth noting that

222501-2

High Intensity $\vec{\gamma}$-Ray Source (HI$\vec{\gamma}$S)

- 直線偏光: 98±2%　[16]
- ビームエネルギー広がり 2-3%　(400-600 keV/20 MeV)
- ビーム強度 1-5×10^7 γ/s

Detector

- NaI(Tl) 10″φ×10″^{L}　4台
- (θ=60 and 120°)× (並行 and 反並行)
- 50.7 msr/detector 、シールド&コリメータあり

標的

- ^{209}Bi 3.1 g/cm^2

Laser Compton Backscattered Photons employing Free Electron Laser

HIγS, Duke, H.R. Weller PPNP62,257(2009), N. Pietralla et al., NIMA483, 556(2002).

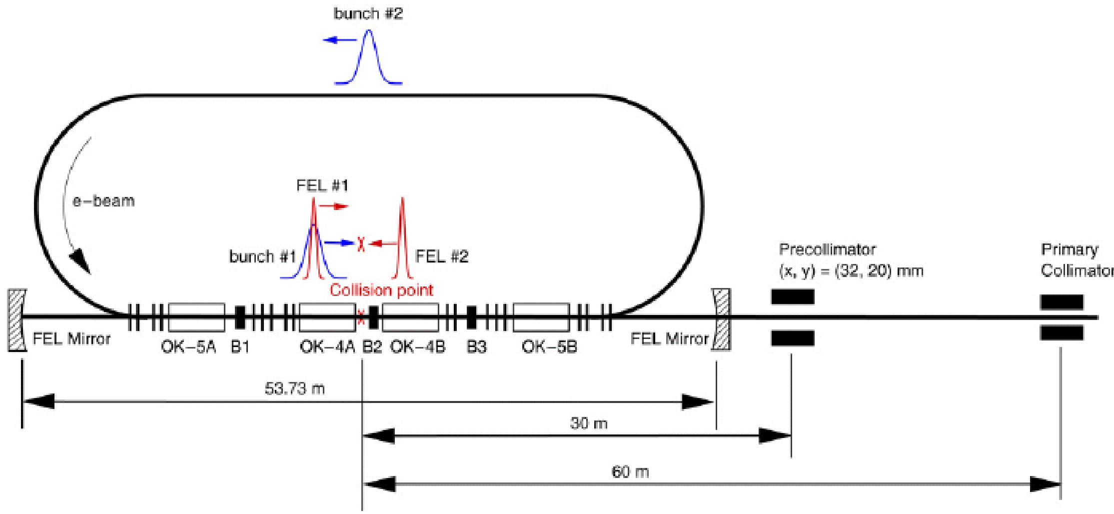

Parameters of high-flux, quasi CW HIγS operation

Parameter	Value	Comments
E-beam configuration	Symmetric two-bunch beam	
E-beam current (mA)	10–80	In two bunches
γ-ray energy, E_γ (MeV)		
With mirrors 1064 to 190 nm	1–84	Available with existing hardware
With 156 nm mirror	85–158	Require FEL and mirror development
Total flux (γ/s)		
(a) No-loss mode (≤20 MeV)		
E_γ = 1–3 MeV	5×10^7–5×10^8 [a]	
E_γ = 3–5 MeV	5×10^8–1×10^9	
E_γ = 5–10 MeV	1×10^9–2×10^9	
E_γ = 10–20 MeV	2×10^9–3×10^9	
(b) Loss mode (>20 MeV)		
E_γ = 21–60 MeV	$>2\times10^8$ [b]	
E_γ = 61–84 MeV	$>1\times10^8$ [b]	190 nm mirror
E_γ = 85–158 MeV	$>1\times10^8$ [c]	156 nm mirror
Linear and circular polarization	>95%	Depending on collimator size

[a] High flux horizontally polarized γ-ray beams can be produced by the OK-4 FEL. The circularly polarized γ-ray flux is low due to the dynamic impact of OK-5 wigglers.
[b] The flux is currently limited by the capability of sustaining a high intracavity power by the FEL mirrors.
[c] Radiation resistive FEL mirrors at 156 nm need to be developed and the FEL wigglers need to be powered at 4000 A.

$$\frac{\Delta E}{E} \sim 3\%$$

$\sim 10^9$ photons/sec

Table 3.1: HI$\vec{\gamma}$S facility operational specifications for $\vec{\gamma}$-ray production. Compared to other Compton facilities in the world HI$\vec{\gamma}$S has the unique combination of high energy tunability, high monoenergetic flux, and high degree of polarization.

Parameter	Value
Location	Durham, NC US
Electron energy (GeV)	0.24-1.2
Laser energy (eV)	1.17-6.53
γ-ray beam energy (MeV)	1-100
Energy Selection	Collimation
Polarization	Linear, Circular
E_γ-resolution (FWHM)	
ΔE (MeV)	0.008-8.5
$\frac{\Delta E}{E}$ (%)	0.8-10
Electron beam current (A)	0.01-0.1
Max on-target flux (γ's/s)	1×10^4-5×10^8
Years of operation	1996-Present

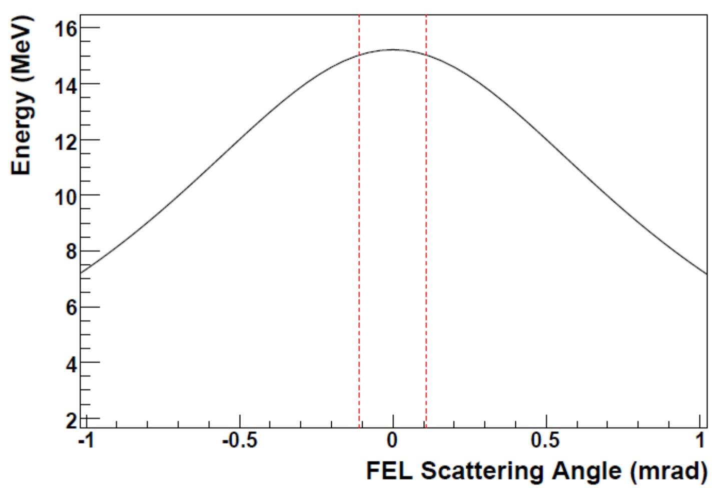

Figure 3.3: The γ-ray energy scattering angle correlation calculated from Equation 3.3. The red dashed lines denote the cutoff of the spectrum resulting from the collimator.

S.S. Henshaw
PhD thesis, 2010

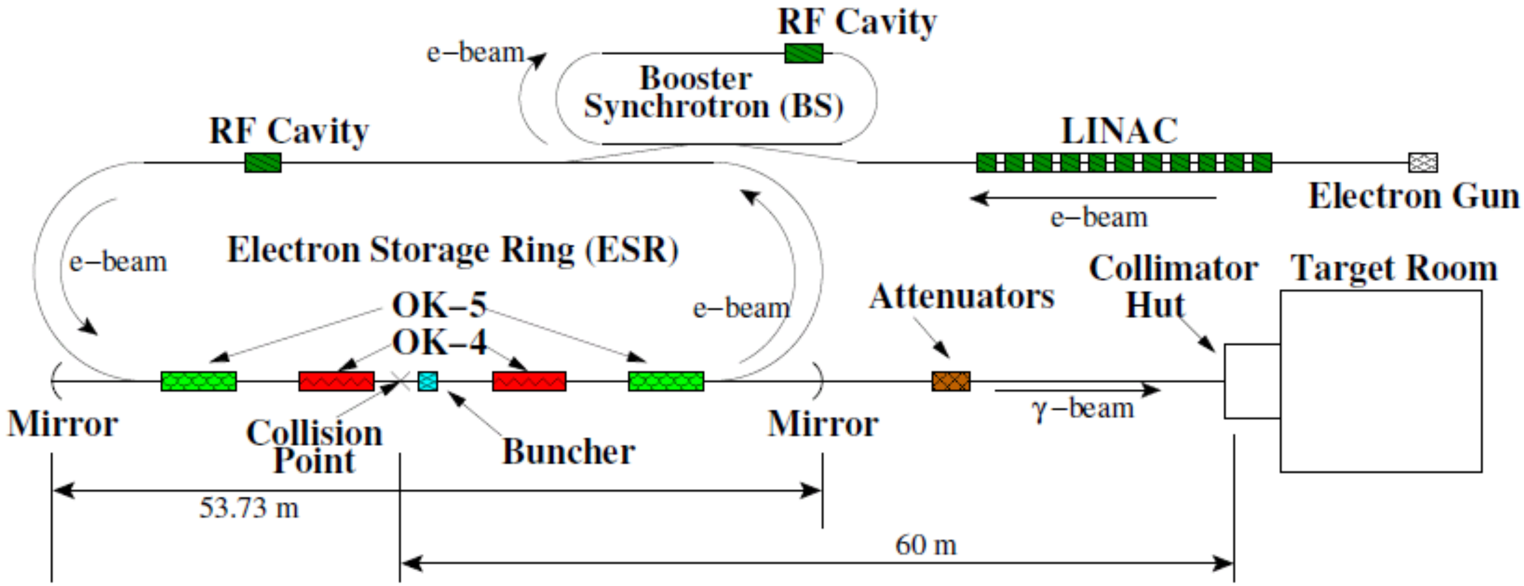

Figure 3.1: Layout of the DFELL. The LINAC injects the electron beam into the BS where it is ramped to the nominal energy of the ESR. Once this energy is reached the electron bunches are injected into the ESR where they travel counterclockwise around the racetrack shape. As the electron bunches enter the OK-4/OK-5 FEL systems FEL photons are generated as well as $\vec{\gamma}$-rays . The $\vec{\gamma}$-rays pass the downstream mirrors, transport to the collimator hut via an evacuated beam pipe, enter the air at the entrance to the collimator hut, and are collimated to the experimental specifications. The $\vec{\gamma}$-rays finally enter the target room where they interact with the target. The $\vec{\gamma}$-rays which do not interact in the target traverse the target room where they are stopped by a 12" thick nickel beam stop.

S.S. Henshaw
PhD thesis, 2010

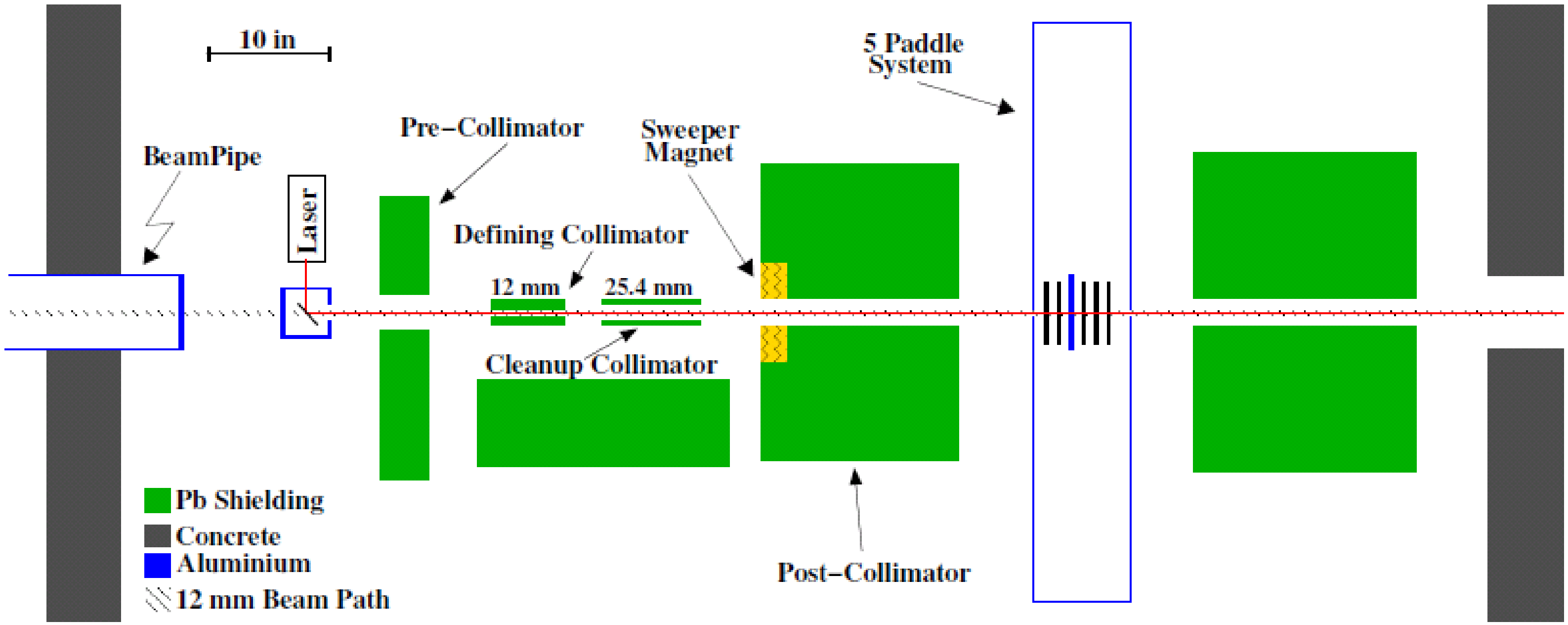

Figure 3.6: Schematic drawing of all the objects contained in the collimator hut. The beam exits the evacuated beampipe and is collimated by the 12mm primary collimator. After exiting the collimator the relative flux of the γ-ray beam is measured using the 5-paddle system.

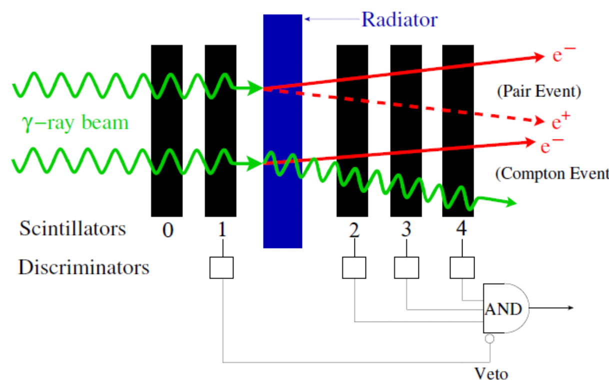

S.S. Henshaw
PhD thesis, 2010

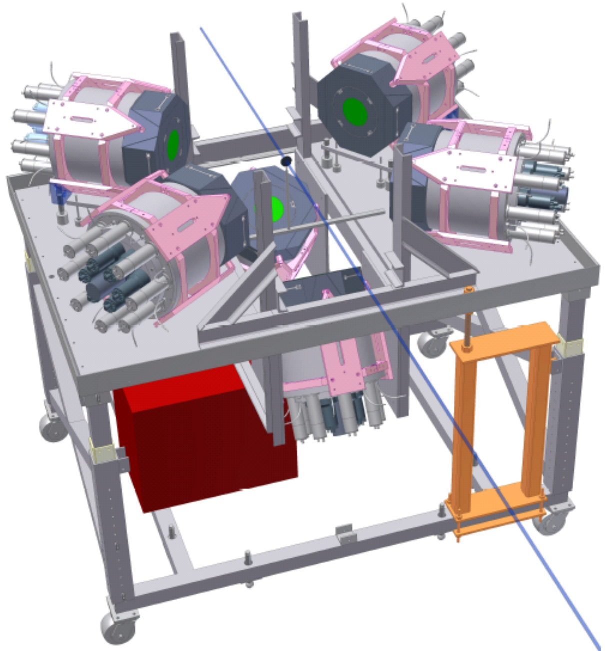

Figure 3.9: Schematic drawing of the HINDA array in the configu
current experiment. The angles and distances to the target for each c
in Table 3.5. Four detectors sit in the plane of polarization and two
it. The blue line represents the path of the incident γ-ray beam.

~100% efficiency
$\Delta E/E$=5-6% at 4.4 MeV

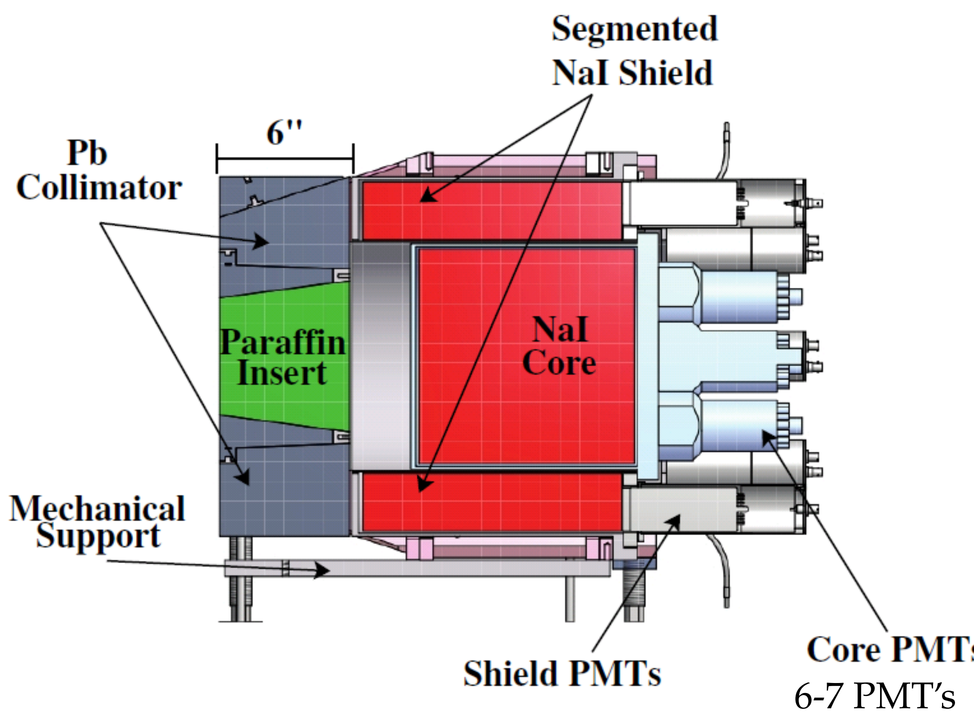

Figure 3.10: A schematic of a HINDA detector assembly. The red section in the center is the core NaI(Tl) crystal, while the red rectangles on top and bottom are the shield NaI(Tl) crystals. The lead shield(grey) defines the solid angle acceptance of the detector. Inside the acceptance of the collimator sits a paraffin plug to reduce neutron capture backgrounds.

S.S. Henshaw
PhD thesis, 2010

TOF

分解能2ns、繰り返し: 179 nsec

正しいタイミングにゲート
偽のタイミングでB.G.を評価して引き算。
(2%)

B.G.（前方角度)

- 指数関数でフィット
- 標的中でのmultistep-atomic process
  (対生成→Bremsstrahlungなど)

分解能

3.5% (at 15.1 MeV)

… 検出器 2.3%、ビーム 2.5%

^{12}C 15.1 MeV gamma

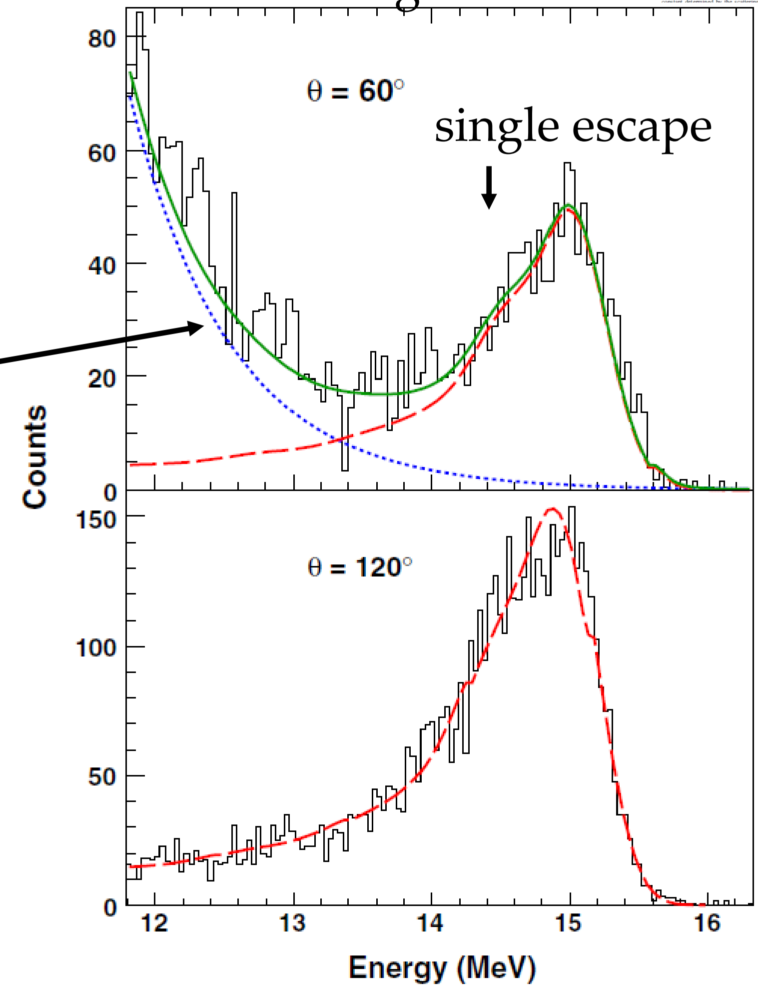

FIG. 1 (color online). NaI(Tl) detector spectra after the applied timing cut at a beam energy of 15.1 MeV. The dashed (red) curves are the simulated detector response functions. The forward-angle spectrum requires an exponential background represented by the dotted (blue) curve to be added to the detector response function, resulting in the solid (green) curve for the total spectrum.

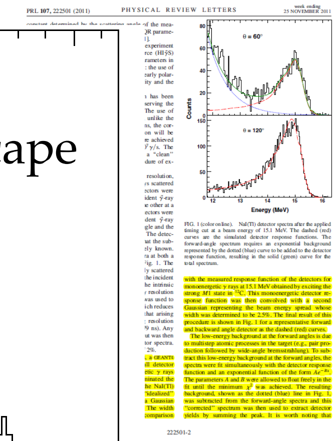

Ex=15-26 MeV、13 点で測定（ビームエネルギー変更）

測定 ~ 80時間

前方と後方で E1-E2 干渉の符号が変わるように角度を選んでいる。

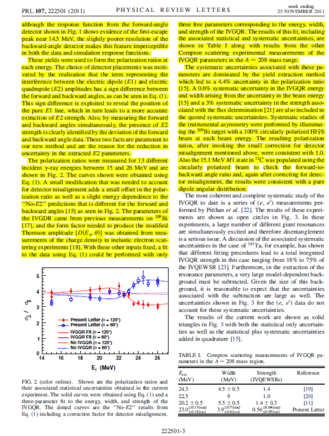

点線は IVGQR がない場合。

→微小なずれ … 検出器のミスアラインメント
→これを補正として取り入れる。

IVGDR のパラメータ
… 前回の実験より[17]

Thomson amplitude
… 電子散乱による電荷密度
分布の値から計算

IVGQR のパラメータ（3つ）
(形はLorentzianでフィット)

・エネルギー

・幅

・ストレングス

さっきの逆数

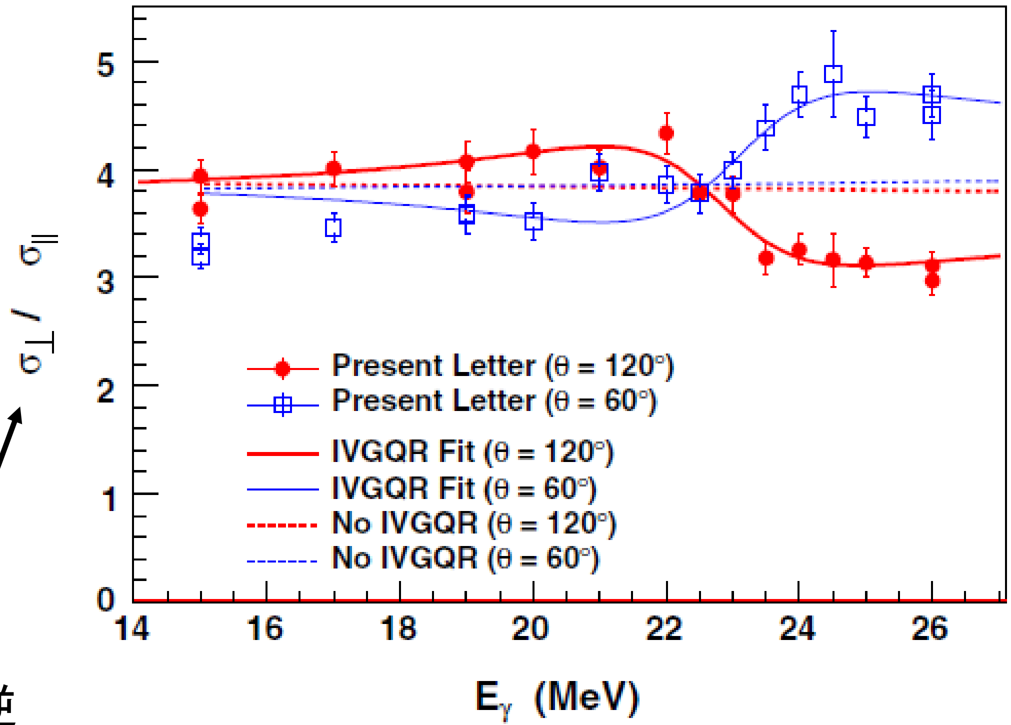

$$\frac{\sigma_\parallel}{\sigma_\perp} = \cos^2\theta + \frac{2|f_{E2}|\cos(\phi_{E2} - \phi_{E1})[\cos^3\theta - \cos\theta]}{|f_{E1} + D(E_\gamma, \theta)|}, \quad (1)$$

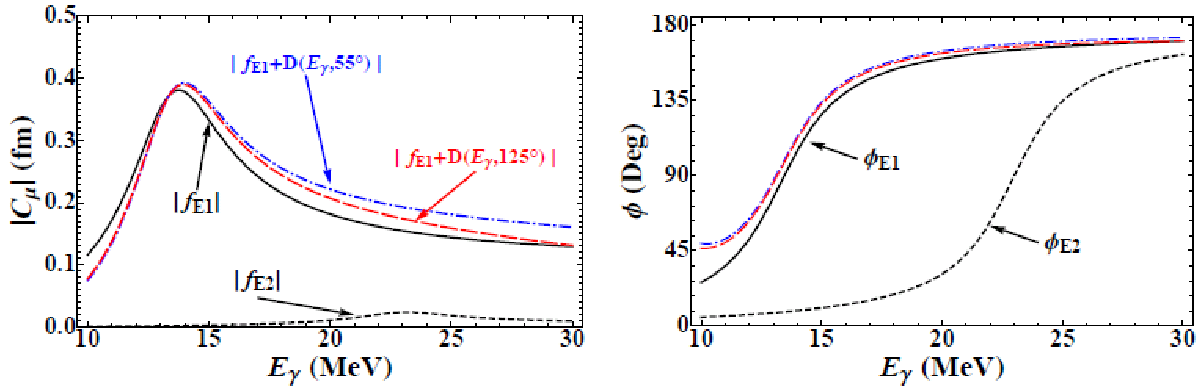

(a) (b)

Figure 2.6: Energy dependence of the forward scattering amplitude's magnitude(a) and phase(b). The blue(dash-dot) and red(dash) curves include the effect of the modified Thomson amplitude on the nuclear $E1$ amplitude at forward(55°) and backward(125°) angles respectively. To generate the curves, Equations 2.12 and 2.16 were inserted into Equation 2.18 and the resonance parameters listed in Table 2.2 were used. To compute the effect of the modified Thomson amplitude the parameters discussed in Section 2.2.1 were used.

$$\Im m[f_\nu^{fi}(E)] = \frac{E}{4\pi\hbar c}\sigma_\gamma^\nu(E)$$

$$\Re e[f_\nu^{fi}(E)] = \frac{1}{4\pi\hbar c}\frac{E_\nu^2 - E^2}{\Gamma_\nu}\sigma_\gamma^\nu(E).$$

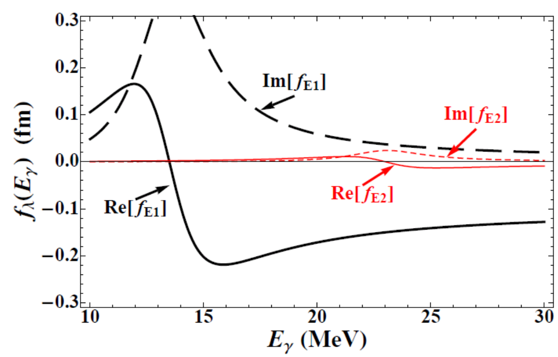

Figure 2.5: Real and imaginary parts of the $E1$ and $E2$ nuclear forward scattering amplitudes as a function of the incident γ-ray energy. $E1$ parameters of Kahane [Kah94] were used, i.e. $E^{E1} = 13.49$ MeV, $\Gamma^{E1} = 3.74$ MeV, and $\sigma_0^{E1} = 693$ mb, which is ~ 1.4 TRK sum rules. $E2$ parameters close to the experimental values were used to generate the resonance curves and have values of: $E^{E2} = 23.0$ MeV, $\Gamma^{E2} = 3.9$ MeV, and $\sigma_0^{E2} = 25.9$ mb, which is approximately 0.75 IVQ-EWSRs, as defined by Equation 1.14.

S.S. Henshaw
PhD thesis, 2010

系統誤差

偏光度比に対して4.4%

IVGDR のエネルギーと幅に対して 0.6% ... ビームエネルギーの不定性 [15]

強度に対して 3% ... ビームfluxの不定性 [21]

・円偏光γ線を使って確認（方位角方向？）

・12C 15.1 MeV の前方・後方比（散乱角方向）を確認

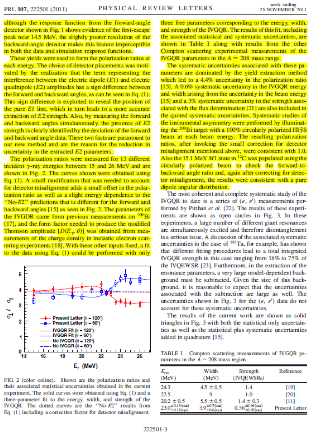

TABLE I. Compton scattering measurements of IVGQR parameters in the $A = 208$ mass region.

E_{res} (MeV)	Width (MeV)	Strength (IVQEWSRs)	Reference
24.3	4.5 ± 0.5	1.4	[19]
22.5	9	1.0	[20]
20.2 ± 0.5	5.5 ± 0.5	1.4 ± 0.3	[11]
$23.0^{\pm 0.13(stat)}_{\pm 0.18(sys)}$	$3.9^{\pm 0.7(stat)}_{\pm 0.6(sys)}$	$0.56^{\pm 0.04(stat)}_{\pm 0.05(sys)}$	Present Letter

IVQEWSR

$$\int \frac{\sigma_\gamma^{E2}(E)}{E^2} dE = \frac{\pi^2}{3} \frac{e^2}{\hbar c} \frac{NZ}{M_n c^2 A} \langle r^2 \rangle \qquad (1.14)$$

電子散乱のデータ[22]と比較。

エラーバーはかなり

ちいさくなった。

特にEx と強度

電子散乱では

他の巨大共鳴との分離により誤差が非常に大きくなっている。

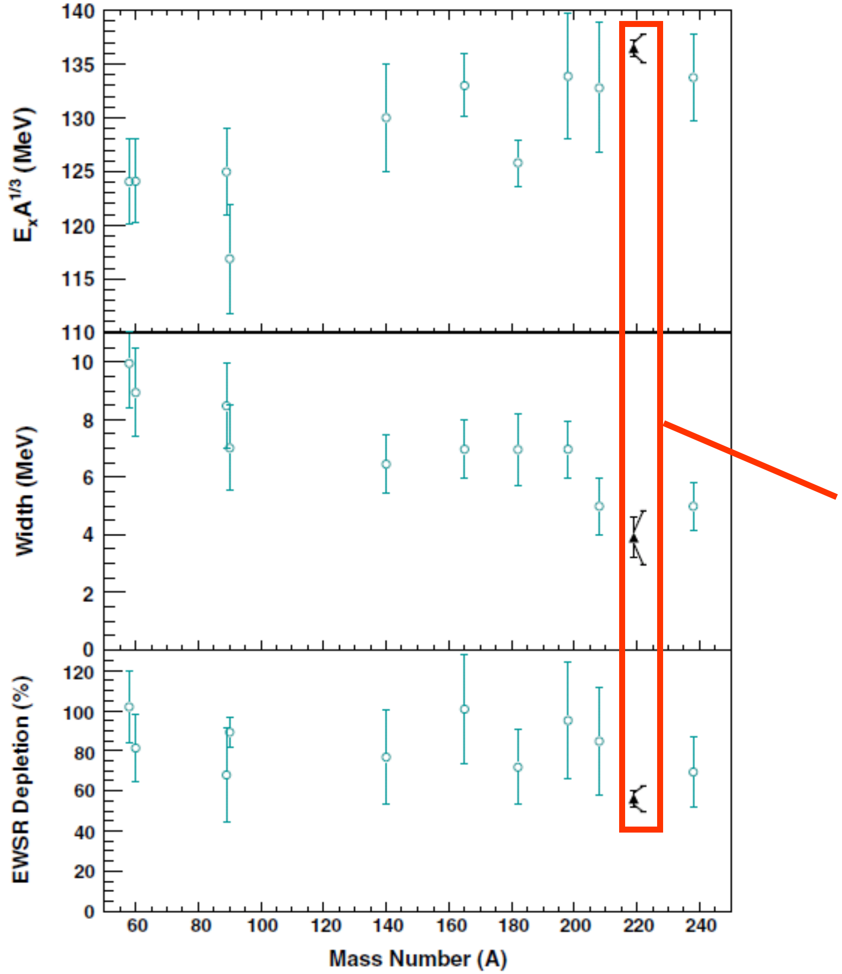

FIG. 3 (color online). The IVGQR parameters and their uncertainties as reported in Pitthan *et al.* [22] are shown as the open (blue) circles here as a function of *A*, along with the present results for ^{209}Bi, shown as solid (black) triangles. For visual clarity, the present ^{209}Bi results have been shifted by 10 mass numbers. Statistical only as well as statistical plus systematic errors are shown for the present results (see text).

今回のデータ。

右へずらしてある。

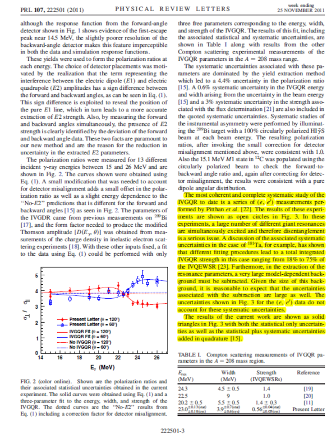

高精度のIVGQRのパラメータが得られた。

・核のsymmetry energy に関する情報が得られるはず。
EoSの特に symmetry energy の密度依存性に関して
強い constraint を与えられるであろう。

→ 中性子星。通常の核物質の~5倍の密度 [10,24]

・さらに他の核にも適用して、系統的に調べるべし。
約 80 時間の測定

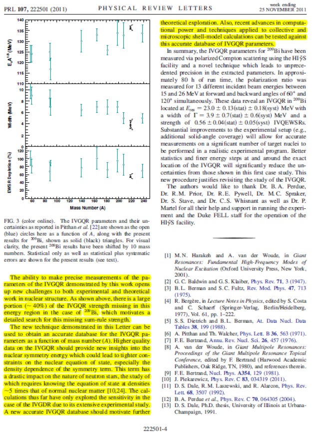
PRL 107, 222501 (2011) PHYSICAL REVIEW LETTERS week ending 25 NOVEMBER 2011

FIG. 3 (color online). The IVGQR parameters and their uncertainties as reported in Pitthan *et al.* [22] are shown as the open (blue) circles here as a function of *A*, along with the present results for ^{209}Bi, shown as solid (black) triangles. For visual clarity, the present ^{209}Bi results have been shifted by 10 mass numbers. Statistical only as well as statistical plus systematic errors are shown for the present results (see text).

The ability to make precise measurements of the parameters of the IVGQR demonstrated by this work opens up new challenges to both experimental and theoretical work in nuclear structure. As shown above, there is a large portion (~ 40%) of the IVGQR strength missing in this energy region in the case of ^{209}Bi, which motivates a detailed search for this missing sum-rule strength.

The new technique demonstrated in this Letter can be used to obtain an accurate database for the IVGQR parameters as a function of mass number (*A*). Higher quality data on the IVGQR should provide new insights into the nuclear symmetry energy which could lead to tighter constraints on the nuclear equation of state, especially the density dependence of the symmetry term. This term has a drastic impact on the nature of neutron stars, the study of which requires knowing the equation of state at densities ~5 times that of normal nuclear matter [10,24]. The calculations thus far have only explored the sensitivity in the case of the IVGDR due to its extensive experimental study. A new accurate IVGQR database should motivate further theoretical exploration. Also, recent advances in computational power and techniques applied to collective and microscopic shell-model calculations can be tested against this accurate database of IVGQR parameters.

In summary, the IVGQR parameters for ^{209}Bi have been measured via polarized Compton scattering using the HI$\vec{\gamma}$S facility and a novel technique which leads to unprecedented precision in the extracted parameters. In approximately 80 h of run time, the polarization ratio was measured for 13 different incident beam energies between 15 and 26 MeV at forward and backward angles of 60° and 120° simultaneously. These data reveal an IVGQR in ^{209}Bi located at $E_{res} = 23.0 \pm 0.13(stat) \pm 0.18(syst)$ MeV with a width of $\Gamma = 3.9 \pm 0.7(stat) \pm 0.6(syst)$ MeV and a strength of $0.56 \pm 0.04(stat) \pm 0.05(syst)$ IVQEWSRs. Substantial improvements to the experimental setup (e.g., additional solid-angle coverage) will allow for accurate measurements on a significant number of target nuclei to be performed in a realistic experimental program. Better statistics and finer energy steps at and around the exact location of the IVGQR will significantly reduce the uncertainties from those shown in this first case study. This new procedure justifies revisiting the study of the IVGQR.

The authors would like to thank Dr. B. A. Perdue, Dr. R.M. Prior, Dr. R.E. Pywell, Dr. M.C. Spraker, Dr. S. Stave, and Dr. C.S. Whisnant as well as Dr. P. Martel for all their help and support in running the experiment and the Duke FELL staff for the operation of the HI$\vec{\gamma}$S facility.

[1] M.N. Harakeh and A. van der Woude, in *Giant Resonances: Fundamental High-Frequency Modes of Nuclear Excitation* (Oxford University Press, New York, 2001).
[2] G.C. Baldwin and G.S. Klaiber, Phys. Rev. **71**, 3 (1947).
[3] B.L. Berman and S.C. Fultz, Rev. Mod. Phys. **47**, 713 (1975).
[4] R. Bergère, in *Lecture Notes in Physics*, edited by S. Costa and C. Schaerf (Springer-Verlag, Berlin/Heidelberg, 1977), Vol. 61, pp. 1–222.
[5] S.S. Dietrich and B.L. Berman, At. Data Nucl. Data Tables **38**, 199 (1988).
[6] A. Pitthan and Th. Walcher, Phys. Lett. B **36**, 563 (1971).
[7] F.E. Bertrand, Annu. Rev. Nucl. Sci. **26**, 457 (1976).
[8] A. van der Woude, in *Giant Multipole Resonances: Proceedings of the Giant Multipole Resonance Topical Conference*, edited by F. Bertrand (Harwood Academic Publishers, Oak Ridge, TN, 1980), and references therein.
[9] F.E. Bertrand, Nucl. Phys. **A354**, 129 (1981).
[10] J. Piekarewicz, Phys. Rev. C **83**, 034319 (2011).
[11] D.S. Dale, R.M. Laszewski, and R. Alarcon, Phys. Rev. Lett. **68**, 3507 (1992).
[12] B.A. Perdue *et al.*, Phys. Rev. C **70**, 064305 (2004).
[13] D.S. Dale, Ph.D. thesis, University of Illinois at Urbana-Champaign, 1991.

222501-4

Isotope Enriched
標的で準備できるも
のは限られていそう…。

Gamma Branch を測定するだけでいいのか？
粒子崩壊との比のEx依存性は？

Summary

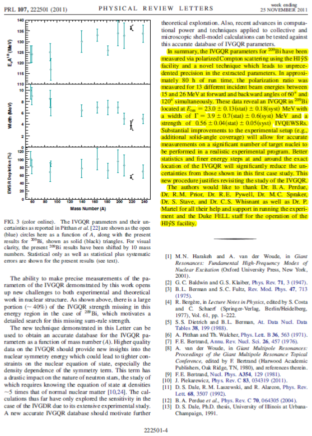

FIG. 3 (color online). The IVGQR parameters and their uncertainties as reported in Pitthan *et al.* [22] are shown as the open (blue) circles here as a function of A, along with the present results for ^{209}Bi, shown as solid (black) triangles. For visual clarity, the present ^{209}Bi results have been shifted by 10 mass numbers. Statistical only as well as statistical plus systematic errors are shown for the present results (see text).

The ability to make precise measurements of the parameters of the IVGQR demonstrated by this work opens up new challenges to both experimental and theoretical work in nuclear structure. As shown above, there is a large portion (~ 40%) of the IVGQR strength missing in this energy region in the case of ^{209}Bi, which motivates a detailed search for this missing sum-rule strength.

The new technique demonstrated in this Letter can be used to obtain an accurate database for the IVGQR parameters as a function of mass number (A). Higher quality data on the IVGQR should provide new insights into the nuclear symmetry energy which could lead to tighter constraints on the nuclear equation of state, especially the density dependence of the symmetry term. This term has a drastic impact on the nature of neutron stars, the study of which requires knowing the equation of state at densities ~5 times that of normal nuclear matter [10,24]. The calculations thus far have only explored the sensitivity in the case of the IVGDR due to its extensive experimental study. A new accurate IVGQR database should motivate further theoretical exploration. Also, recent advances in computational power and techniques applied to collective and microscopic shell-model calculations can be tested against this accurate database of IVGQR parameters.

In summary, the IVGQR parameters for ^{209}Bi have been measured via polarized Compton scattering using the HI$\vec{\gamma}$S facility and a novel technique which leads to unprecedented precision in the extracted parameters. In approximately 80 h of run time, the polarization ratio was measured for 13 different incident beam energies between 15 and 26 MeV at forward and backward angles of 60° and 120° simultaneously. These data reveal an IVGQR in ^{209}Bi located at $E_{res} = 23.0 \pm 0.13(\text{stat}) \pm 0.18(\text{syst})$ MeV with a width of $\Gamma = 3.9 \pm 0.7(\text{stat}) \pm 0.6(\text{syst})$ MeV and a strength of $0.56 \pm 0.04(\text{stat}) \pm 0.05(\text{syst})$ IVQEWSRs. Substantial improvements to the experimental setup (e.g., additional solid-angle coverage) will allow for accurate measurements on a significant number of target nuclei to be performed in a realistic experimental program. Better statistics and finer energy steps at and around the exact location of the IVGQR will significantly reduce the uncertainties from those shown in this first case study. This new procedure justifies revisiting the study of the IVGQR.

The authors would like to thank Dr. B. A. Perdue, Dr. R.M. Prior, Dr. R.E. Pywell, Dr. M.C. Spraker, Dr. S. Stave, and Dr. C.S. Whisnant as well as Dr. P. Martel for all their help and support in running the experiment and the Duke FELL staff for the operation of the HI$\vec{\gamma}$S facility.

[1] M.N. Harakeh and A. van der Woude, in *Giant Resonances: Fundamental High-Frequency Modes of Nuclear Excitation* (Oxford University Press, New York, 2001).
[2] G. C. Baldwin and G.S. Klaiber, Phys. Rev. **71**, 3 (1947).
[3] B.L. Berman and S.C. Fultz, Rev. Mod. Phys. **47**, 713 (1975).
[4] R. Bergère, in *Lecture Notes in Physics*, edited by S. Costa and C. Schaerf (Springer-Verlag, Berlin/Heidelberg, 1977), Vol. 61, pp. 1–222.
[5] S.S. Dietrich and B.L. Berman, At. Data Nucl. Data Tables **38**, 199 (1988).
[6] A. Pitthan and Th. Walcher, Phys. Lett. B **36**, 563 (1971).
[7] F.E. Bertrand, Annu. Rev. Nucl. Sci. **26**, 457 (1976).
[8] A. van der Woude, in *Giant Multipole Resonances: Proceedings of the Giant Multipole Resonance Topical Conference*, edited by F. Bertrand (Harwood Academic Publishers, Oak Ridge, TN, 1980), and references therein.
[9] F.E. Bertrand, Nucl. Phys. **A354**, 129 (1981).
[10] J. Piekarewicz, Phys. Rev. C **83**, 034319 (2011).
[11] D. S. Dale, R.M. Laszewski, and R. Alarcon, Phys. Rev. Lett. **68**, 3507 (1992).
[12] B. A. Perdue *et al.*, Phys. Rev. C **70**, 064305 (2004).
[13] D. S. Dale, Ph.D. thesis, University of Illinois at Urbana-Champaign, 1991.

励起強度分布のモーメントと和則

オペレータFに対する励起強度関数（Strength Function）

$$S(\omega) \equiv \sum_k \left| \langle k | F | 0 \rangle \right|^2 \delta(\omega - \omega_k)$$

ω: 励起エネルギー

励起強度関数S(ω)のp次のモーメント

$$m_p \equiv \int_0^\infty S(\omega) \omega^p d\omega = \sum_k \left| \langle k | F | 0 \rangle \right|^2 \omega_k^p$$

参考文献[8]

$$S = m_0 = \int_0^{\infty} S(\omega)d\omega = \sum_k \left|\langle k|F|0\rangle\right|^2$$

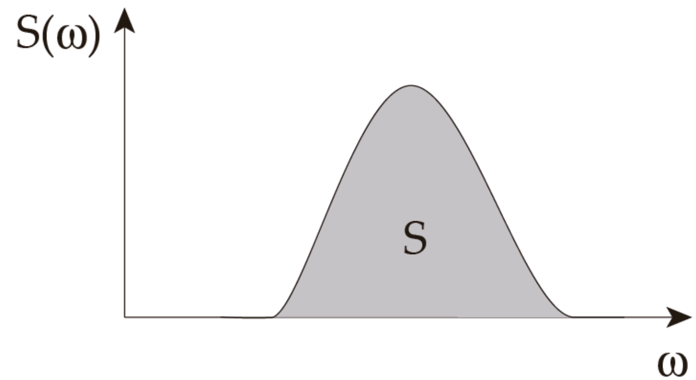

$$\overline{\omega} = \frac{m_1}{m_0} = \frac{\int_0^{\infty} S(\omega)\omega\ d\omega}{\int_0^{\infty} S(\omega)d\omega} = \frac{\sum_k \left|\langle k|F|0\rangle\right|^2 \omega_k}{\sum_k \left|\langle k|F|0\rangle\right|^2}$$

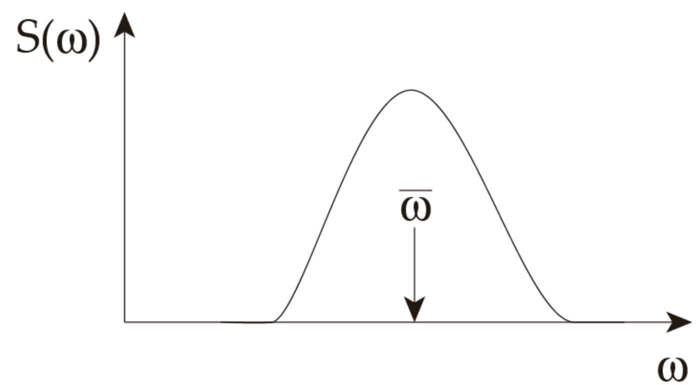

$$\sigma^2 = \frac{m_2}{m_0} - \left(\frac{m_1}{m_0}\right)^2 = \frac{\int_0^{\infty} S(\omega)\omega^2 d\omega}{\int_0^{\infty} S(\omega)d\omega} - \left(\frac{\int_0^{\infty} S(\omega)\omega d\omega}{\int_0^{\infty} S(\omega)d\omega}\right)^2$$

$$= \frac{\int_0^{\infty} S(\omega)(\omega - \overline{\omega})^2 d\omega}{\int_0^{\infty} S(\omega)d\omega}$$

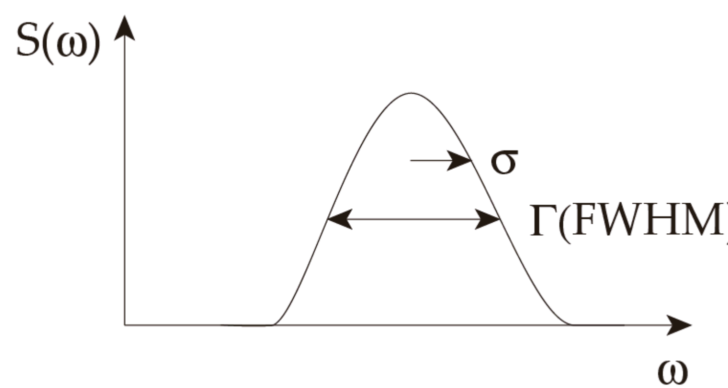

参考文献[8]

全ての励起状態に関する積算値は、
対応するオペレータの
基底状態の期待値を表す。

$F : Hermitian$

$F = F^{\dagger}$

$$
\begin{aligned}
m_p \equiv \int_0^{\infty} S(\omega)\omega^p d\omega &= \sum_k \left| \langle k | F | 0 \rangle \right|^2 \omega_k^p \\
&= \sum_k \langle 0 | F | k \rangle \langle k | F | 0 \rangle \omega_k^p \\
&= \langle 0 | F \left(\sum_k | k \rangle \langle k | \right) \omega_k^p F | 0 \rangle \\
&= \langle 0 | F (H - E_0)^p F | 0 \rangle
\end{aligned}
$$

励起状態を全て調べると基底状態の性質が分かる。

参考文献[8]

対応するオペレータは、ハミルトニアンHとの（反）交換関係で表すことができる（ことがある）。

$$m_0 = \frac{1}{2}\langle 0 | F^2 | 0 \rangle$$

$$m_1 = \frac{1}{2}\langle 0 | [F,[H,F]] | 0 \rangle$$

$$m_2 = \frac{1}{2}\langle 0 | \{[F,H],[H,F]\} | 0 \rangle$$

$$m_3 = \frac{1}{2}\langle 0 | [[F,H],[H,[H,F]]] | 0 \rangle$$

導出例:

$$\begin{aligned} m_1 &= \frac{1}{2}\langle 0 | [F,[H,F]] | 0 \rangle \\ &= \frac{1}{2}\langle 0 | [F, HF - FH] | 0 \rangle \\ &= \frac{1}{2}\langle 0 | FHF - F^2 H - HF^2 + FHF] | 0 \rangle \\ &= \frac{1}{2}\langle 0 | 2FHF - F^2 E_0 - E_0 F^2] | 0 \rangle \\ &= \langle 0 | F (H - E_0)^1 F | 0 \rangle \end{aligned}$$

参考文献[8]

参考文献[5]

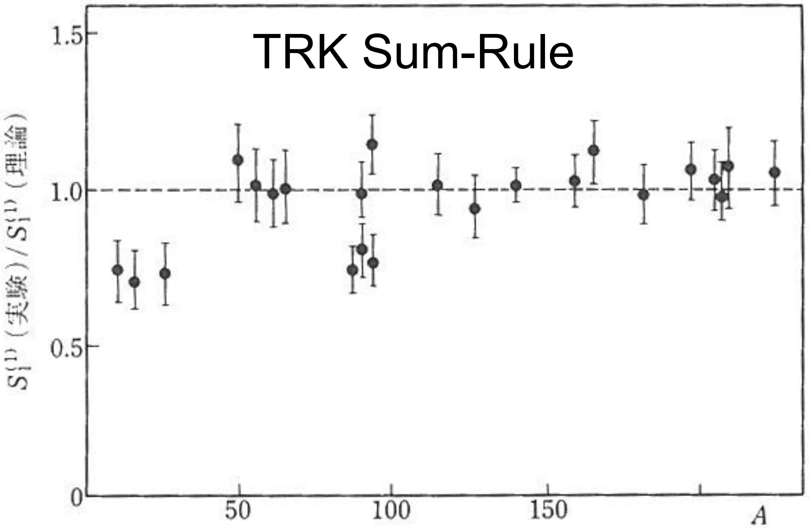

図 3.1　1⁻ 状態励起に対する和則値の理論値と実験値の比[8]
実験値は励起エネルギー30 MeV までの和．A は原子核の質量数

参考文献[5]

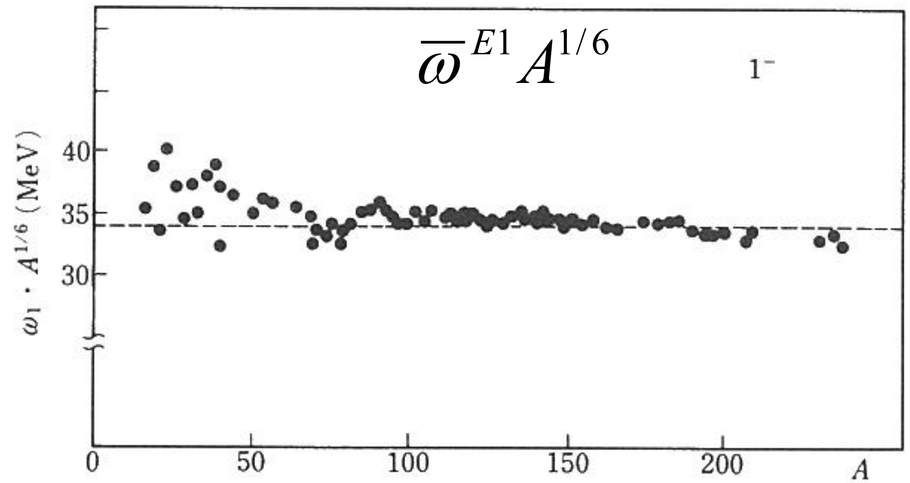

図 3.3　1⁻ 巨大共鳴状態のエネルギー ω_1 の質量数(A)依存[9](実験値(●)は $\omega_1=34/A^{1/6}$(MeV)でよく再現される)

参考文献[6]

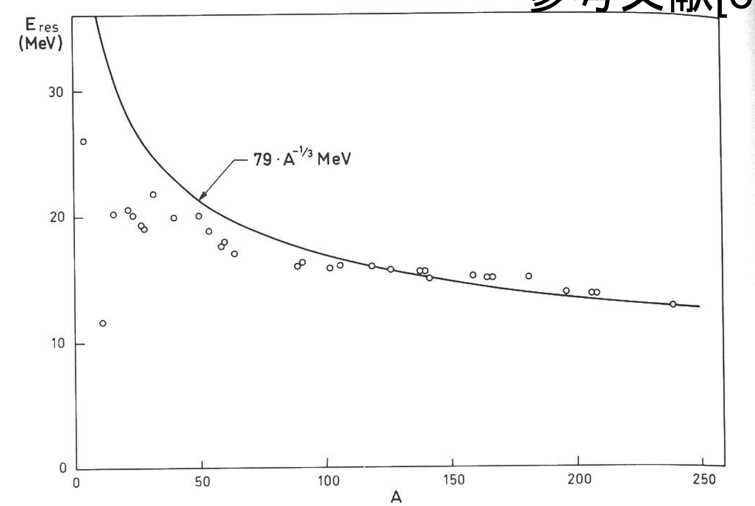

Figure 6-19 Systematics of dipole resonance frequency. The experimental data are taken from the review article by E. Hayward (*Nuclear Structure and Electromagnetic Interactions*, p. 141, ed. N. MacDonald, Oliver and Boyd, Edinburgh and London, 1965), except for ^{4}He, for which the resonance frequency is that given in the survey article by W. E. Meyerhof and T. A. Tombrello, *Nuclear Phys.* **A109**, 1 (1968). In the case of the deformed nuclei, which exhibit two resonance maxima, the energy represents a weighted mean of the two resonance energies. The solid curve represents the estimate based on the liquid-drop model (see Eq. (6A-65)).

Symmetry Energy に、**Volumeの効果とSurfaceの効果を両方とりいれる必要**がある。

Surface効果には中性子スキンが大きく寄与する。